Effective interactions in shell-model calculations

2003. 9. 19 CISS03

M. Honma (Univ. of Aizu)
T. Mizusaki (Senshu Univ.)
T. Otsuka (Univ. of Tokyo/RIKEN)
B. A. Brown (MSU)

Outline

- Introduction
- Problems in microscopic effective interaction
- Monopole correction
- Beyond-monopole correction
- Summary

Nuclear shell-model

- Powerful tool for the study of nuclear structure
  - Unified treatment of single-particle and collective motions
  - Systematic description over wide mass range
  - Prediction / indication of new physics
- Key … effective interaction

Model space

- Closed core + valence shell
- $0\hbar\omega$ space

  p-shell ^{4}He + $0p_{3/2}$, $0p_{1/2}$

  sd-shell ^{16}O + $0d_{5/2}$, $1s_{1/2}$, $0d_{3/2}$

  pf-shell ^{40}Ca + $0f_{7/2}$, $1p_{3/2}$, $1p_{1/2}$, $0f_{5/2}$

  …
- $n\hbar\omega$ space

  p-sd, sd-pf, …

  For unstable nuclei, large deformation, …
- No-core shell model

  Few-body ~ light nuclei

Hamiltonian

Nucleons in a mean potential interacting through residual interactions

- Single particle energy (SPE)
- Two-body interaction (TBME)

$$H = \sum_a \varepsilon_a n_a + \sum_{a\le b, c\le d, JT} V(abcd; JT) A^+_{JT}(ab) A_{JT}(cd)$$

n_a … number operators of orbit a

$$A^\dagger_{abJT} = (1+\delta_{ab})^{-1/2} \left[c^\dagger_a c^\dagger_b \right]^{JT}$$

Effective interaction

- Microscopic (realistic)
  - Derived from NN-interaction
  - Problems for many valence nucleons
- Empirical
  - Fit to experimental data

    Feasible only for small shells (e.g. CK for *p*-shell)
  - Potential model
- Semi-empirical
  - Modify microscopic TBME empirically

pf-shell

- Current frontier of shell model calculations
- Single-particle vs. collective
- Protons & neutrons occupy the same shell

  pn-interaction
- Spin-orbit splitting

  N, *Z*=28 magic number

  "soft" ^{56}Ni core ⟶ active 2-shell problem
- Astrophysics

  Electron capture rate

Shell model calculations

- Limitation due to huge dimension of Hamiltonian matrix

  ex. $M = 0$ dim. $\sim 2\times10^9$ for ^{60}Zn

- Conventional Lanczos diagonalization
  - Feasible up to $\sim 10^8$
  - Truncation of model space: $(f_{7/2})^{n_1-t}(p_{3/2}\ f_{5/2}\ p_{1/2})^{n_2+t}$
  - $t \sim 5$ calculation is possible for most pf-shell nuclei

    sufficient for low-lying configurations

    fails for describing significant core-excitations

    (ex. 4p-4h band in ^{56}Ni)

Monte Carlo shell model

Review: T. Otsuka et al., Prog. Part. Nucl. Phys. 47 (2001) 319

- Deformed Slater determinant bases

$$|\phi\rangle = \prod_\alpha a_\alpha^\dagger |0\rangle, \qquad a_\alpha^\dagger = \sum_i c_i^\dagger D_{i\alpha} \quad (\, c_i^\dagger \ldots \text{HO basis})$$

- Monte Carlo basis generation

$$|\phi(\sigma)\rangle = \prod_n e^{-\Delta\beta h(\vec{\sigma}_n)} |\phi\rangle$$

$$h(\sigma_n) = h_{HF} + \sum_\alpha \sigma_{\alpha n} O_\alpha \qquad \text{one-body Hamiltonian } (\leftarrow H\,)$$

$\boldsymbol{\sigma}$ … auxiliary field (random variable)

- Symmetry restoration by projection
- Basis selection by energy gain

(importance truncation)

- Variational basis improvement

$$\sigma \to \sigma + \delta\sigma$$

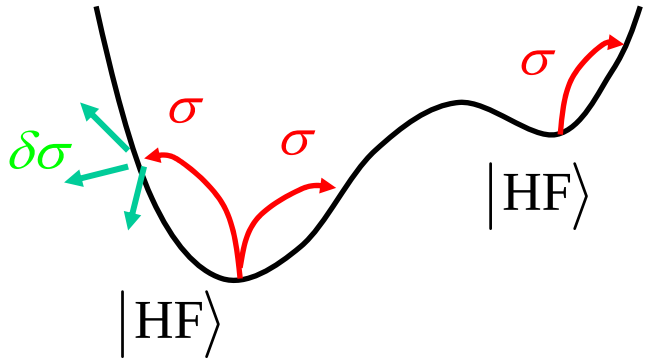

Few-dimensional approximation

- MCSM wave function is dominated by only a few bases
  - Taking only a few bases from local energy minima (FDA)
  - Optimum 1st basis = *J*-projected HF state
  - Typical error < ~1 MeV
- Empirical corrections
  - Extrapolation from solvable problems
  - Corrections depend on the *J*-shceme dimension (FDA*)

Realistic effective interaction

- Derived from NN-potential
  - Renormalized G-matrix
- Examples
  - KB … T.T.S.Kuo and G.E.Brown Nucl. Phys. A114 (1968) 241
    - Hamada-Johnston potential
    - Renormalization due to core-polalization
  - G … M. Hjorth-Jensen, et al., Phys. Repts. 261 (1995) 125
    - Bonn-C potential
    - 3rd order Q-box + folded diagram

KB interaction

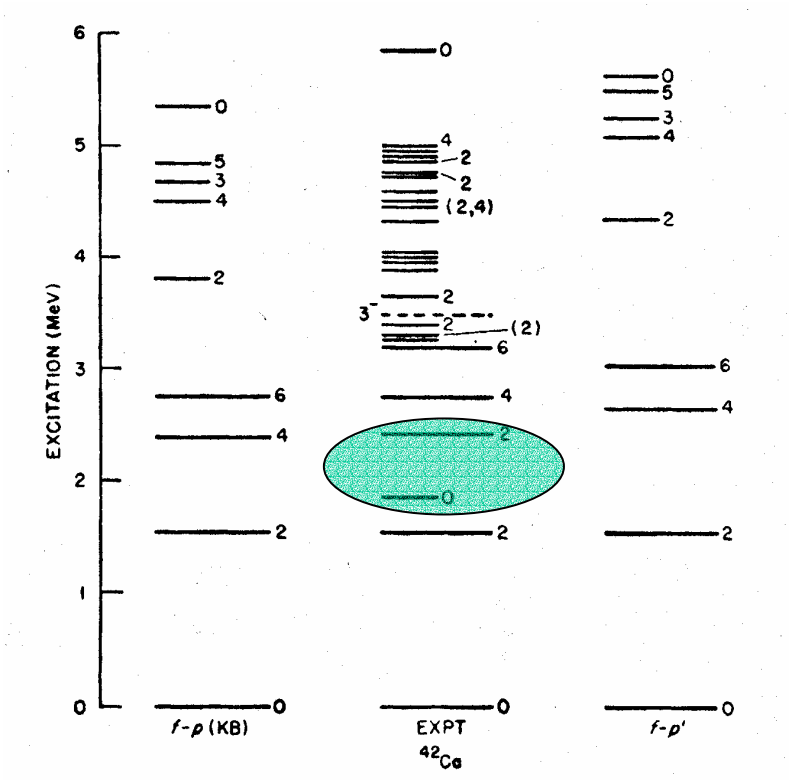

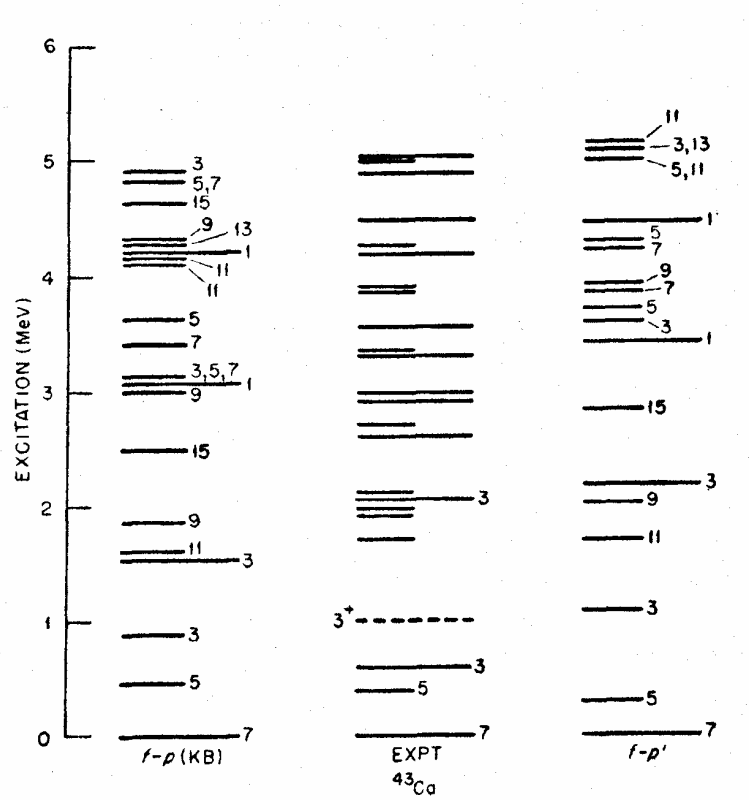

J. B. McGrory et al., Phys. Rev. C2 (1970) 186

KB interaction

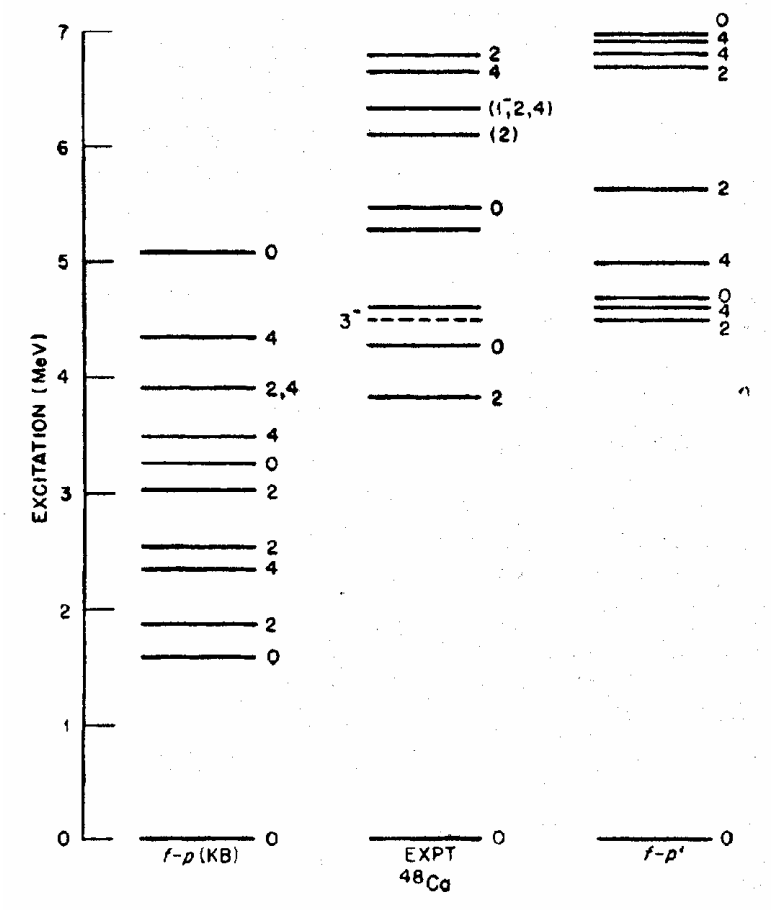

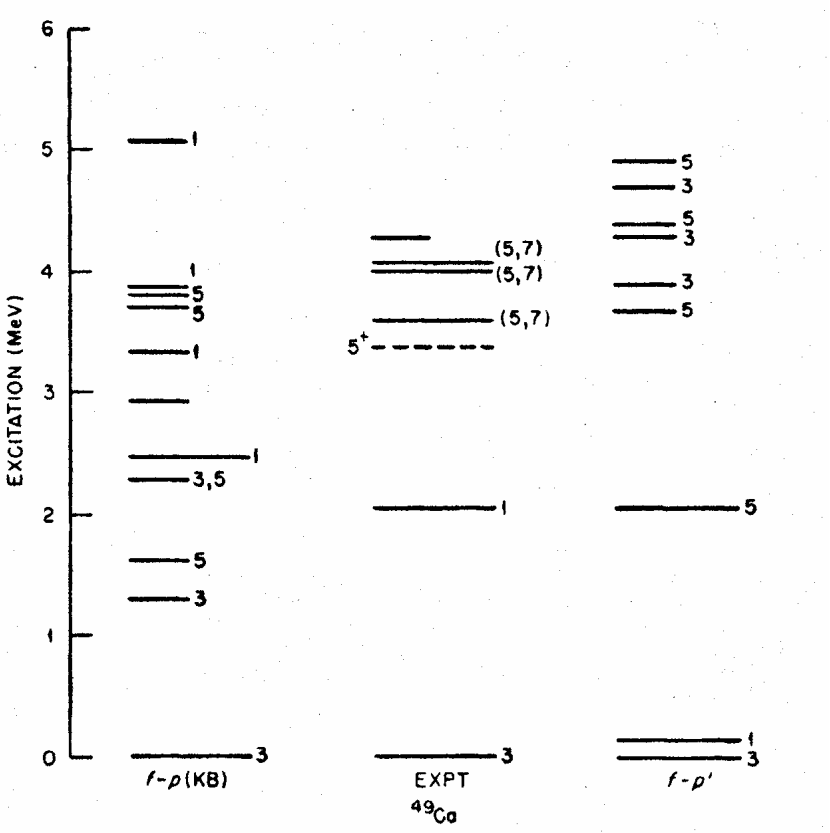

G interaction

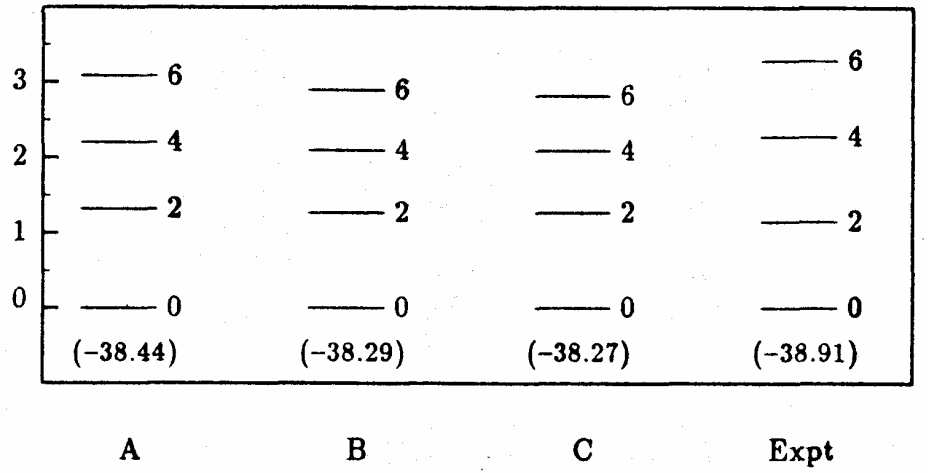

Fig. 51. The low-lying ^{44}Ca spectra relative to ^{40}Ca.

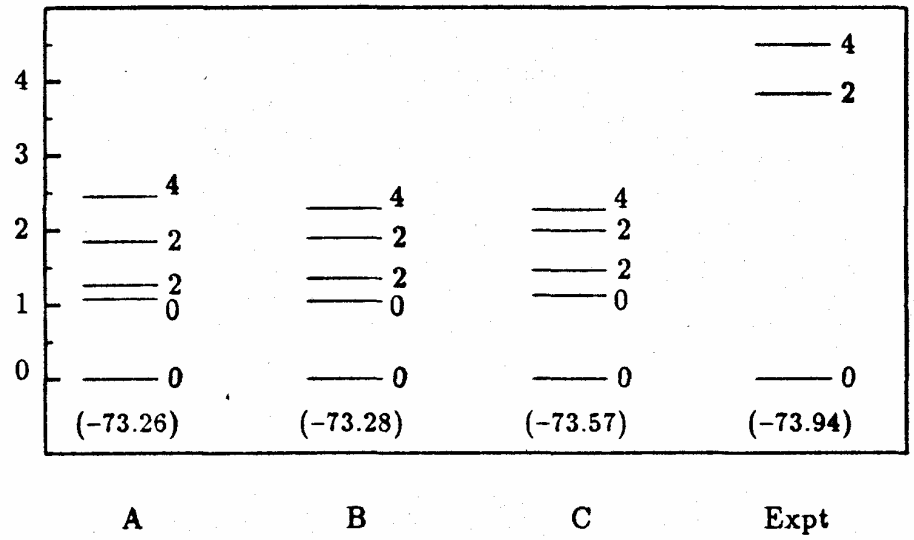

Fig. 56. The low-lying ^{48}Ca spectra relative to ^{40}Ca.

M. Hjorth-Jensen et al.,
Phys. Repts. 261 (1995) 125

G interaction

FDA*

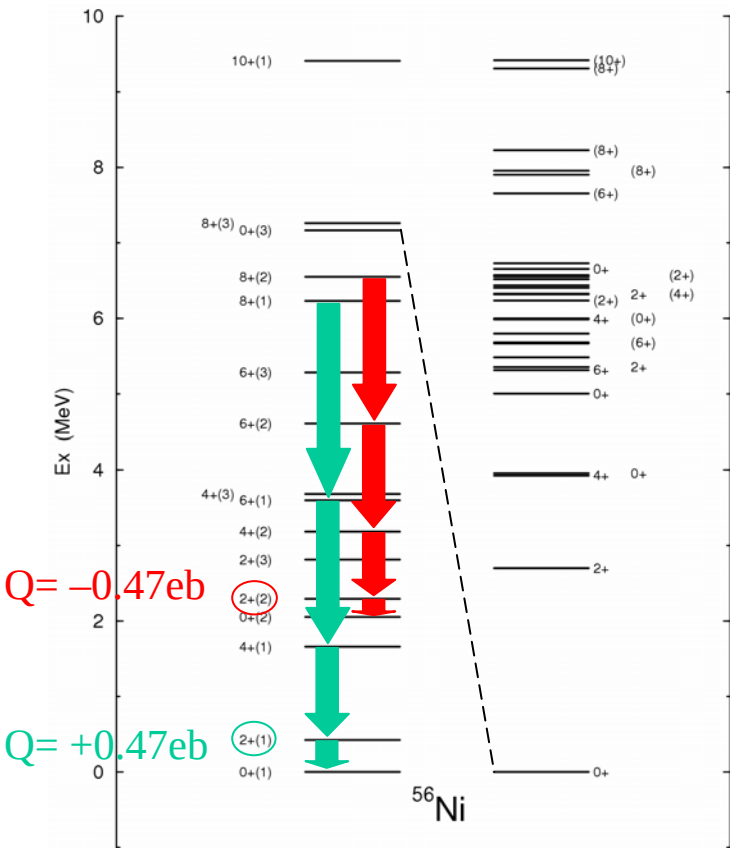

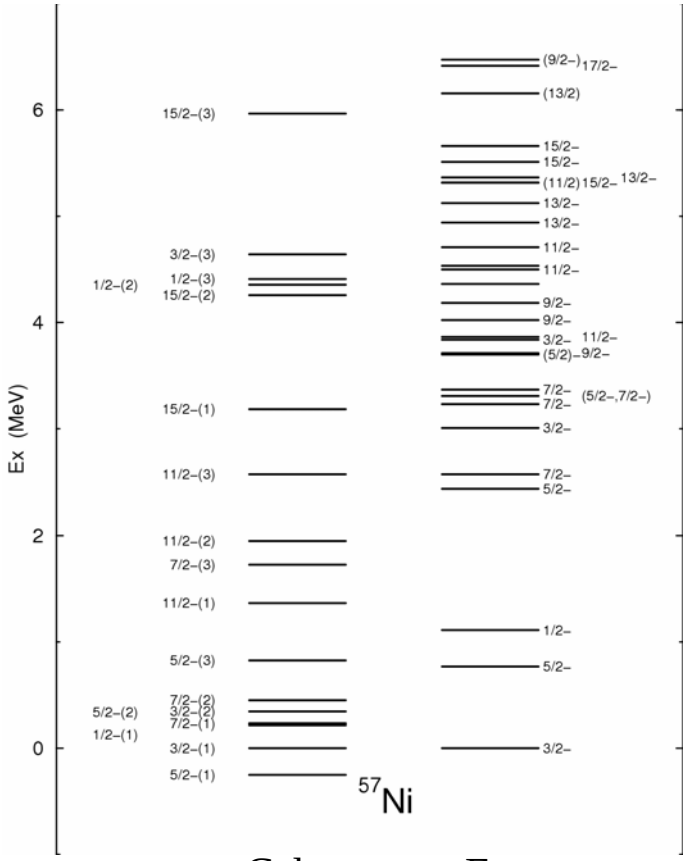

Empirical modifications

- KB’ by McGrory et al.

$$\left\langle f_{7/2}^2 J \left| V \right| f_{7/2}^2 J \right\rangle \quad \Rightarrow \quad -300\text{keV for } J = 0, 2$$

$$\left\langle f_{7/2} p_{3/2} J \left| V \right| f_{7/2} p_{3/2} J \right\rangle \quad \Rightarrow \quad +300\text{keV}$$

Monopole Hamiltonian

- Determines average energy of eigenstates in a given configuration.
  - Important for binding energies, shell gaps

$$H_m = \sum_a \varepsilon_a n_a + \sum_{a \le b} \frac{1}{1+\delta_{ab}} \left[\frac{3V_{ab}^1 + V_{ab}^0}{4} n_a (n_a - \delta_{ab}) + (V_{ab}^1 - V_{ab}^0)(T_a \cdot T_b - \frac{3}{4} n_a \delta_{ab}) \right]$$

n_a, T_a … number, isospin operators of orbit a

- Monople centroids
  - Angular-momentum averaged effects of two-body interaction

$$V_{ab}^T = \frac{\sum_J (2J+1) V_{abab}^{JT}}{\sum_J (2J+1)}$$

KB3 interaction

A. Poves and A. P. Zuker, Phys. Repts. 70 (1981) 235

- KB’

$$V^T_{fr}(\mathrm{KB}') = V^T_{fr}(\mathrm{KB}) - (-)^T\, 300\mathrm{keV}$$

$f \ldots f_{7/2}\,, \qquad r \ldots p_{3/2}, f_{5/2}, p_{1/2}$

- KB1

$$V^0_{ff}(\mathrm{KB1}) = V^0_{ff}(\mathrm{KB}) - 350\mathrm{keV}$$

$$V^1_{ff}(\mathrm{KB1}) = V^1_{ff}(\mathrm{KB}) - 110\mathrm{keV}$$

- KB3

$$V^{J0}_{ffff}(\mathrm{KB3}) = V^{J0}_{ffff}(\mathrm{KB1}) - 300\mathrm{keV} \quad \text{for } J = 1, 3$$

$$V^{21}_{ffff}(\mathrm{KB3}) = V^{21}_{ffff}(\mathrm{KB1}) - 200\mathrm{keV}$$

Other matrix elements are modified so as to keep the KB1 centroids

KB3

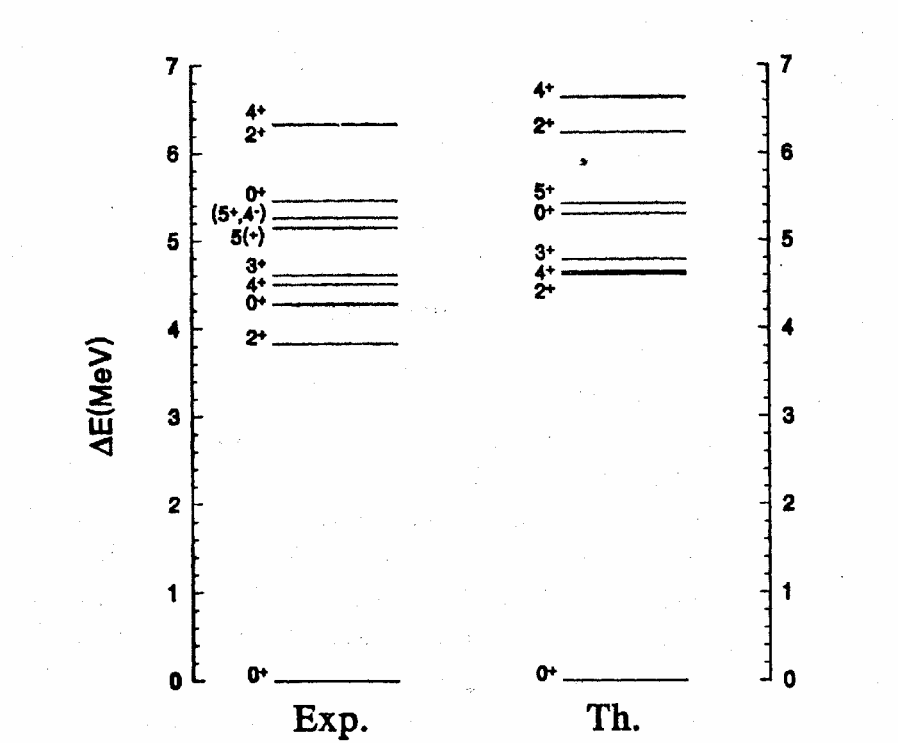

FIG. 1. Experimental and theoretical energy levels of ^{48}Ca.

E. Caurier et al., PRC50 (1994) 225

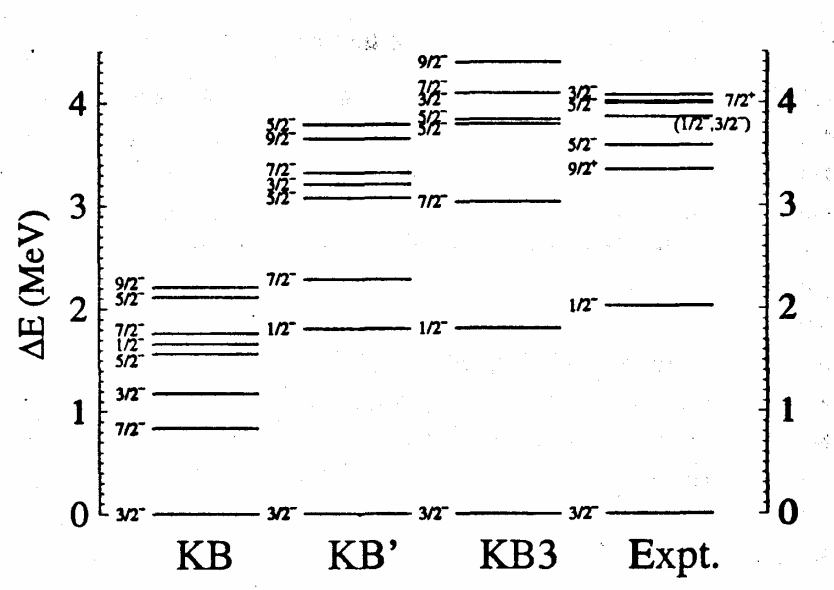

FIG. 12. Theoretical levels for the KB, KB′, and KB3 interactions compared with experiment in ^{49}Ca.

G. Martinez-Pinedo, et al., PRC55 (1997) 187

KB3

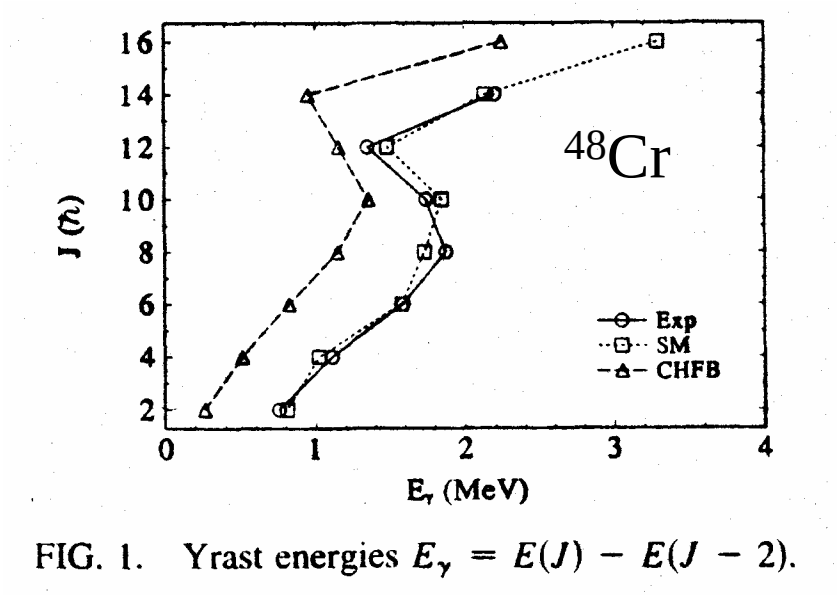

FIG. 1. Yrast energies $E_\gamma = E(J) - E(J-2)$.

E. Caurier et al., PRL75 (1995) 2466

^{52}Fe

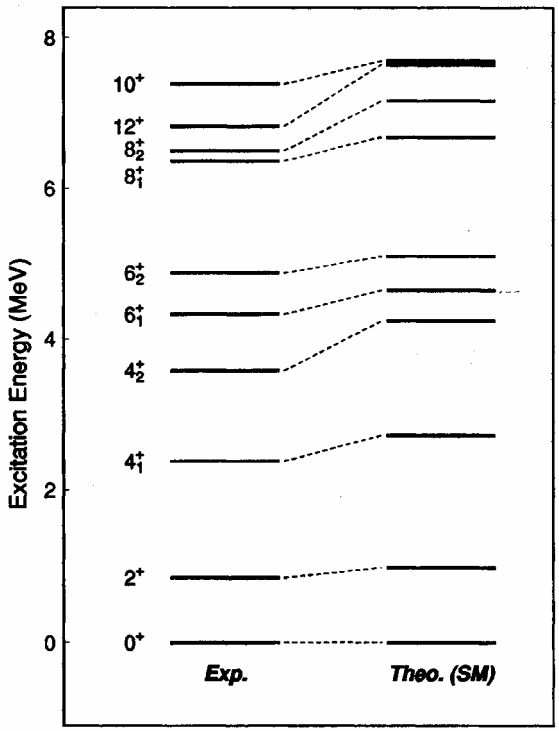

FIG. 5. Comparison between the experimental and the shell model positive parity energy levels in ^{52}Fe. Dashed lines connect the experimental levels with their calculated counterpartners.

C. A. Ur et al., PRC58 (1998) 3163

KB3

FDA*

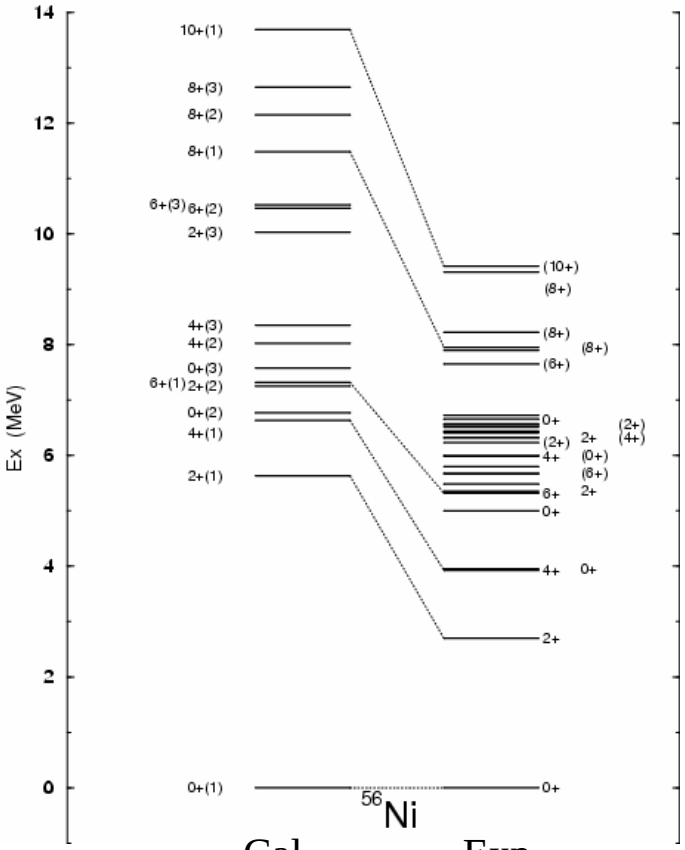
Ex (MeV)
14
12
10
8
6
4
2
0
10+(1)
8+(3)
8+(2)
8+(1)
6+(3)
6+(2)
2+(3)
4+(3)
4+(2)
0+(3)
6+(1)
2+(2)
0+(2)
4+(1)
2+(1)
0+(1)
(10+)
(8+)
(8+)
(8+)
(6+)
0+
(2+)
4+
6+
0+
4+
2+
0+
2+
(2+)
(4+)
(0+)
(6+)
2+
0+
56Ni
Cal.
Exp.

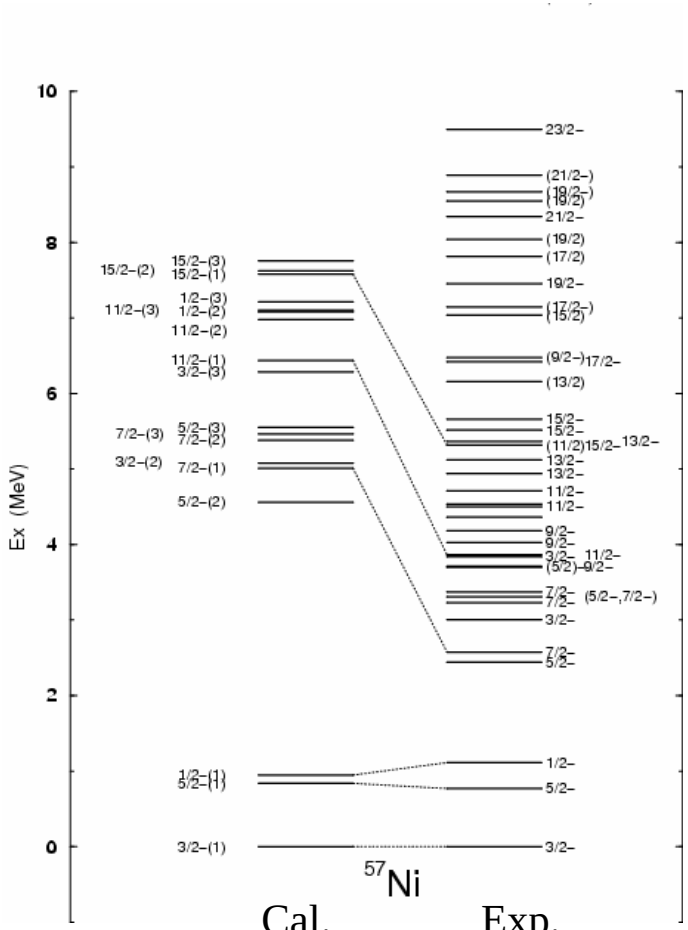
Ex (MeV)
10
8
6
4
2
0
15/2−(2)
15/2−(3)
15/2−(1)
11/2−(3)
1/2−(3)
1/2−(2)
11/2−(2)
11/2−(1)
3/2−(3)
7/2−(3)
5/2−(3)
7/2−(2)
3/2−(2)
7/2−(1)
5/2−(2)
1/2−(1)
5/2−(1)
3/2−(1)
23/2−
(21/2−)
(19/2−)
(18/2)
21/2−
(19/2)
(17/2)
19/2−
(17/2−)
(15/2)
(9/2−)17/2−
(13/2)
15/2−
15/2−
(11/2)15/2−13/2−
13/2−
13/2−
11/2−
11/2−
9/2−
9/2−
9/2− 11/2−
(5/2)−9/2−
7/2− (5/2−,7/2−)
7/2−
3/2−
7/2−
5/2−
1/2−
5/2−
3/2−
57Ni
Cal.
Exp.

Shell gap

Modify KB3 to fit the shell gap for ^{56}Ni ⟶ KB3G

A. Poves et al., NPA694 (2001) 157

$$V^0_{fp}(\text{KB3G}) = V^0_{fp}(\text{KB3}) - 100\text{keV}, \quad V^1_{fp}(\text{KB3G}) = V^1_{fp}(\text{KB3}) - 50\text{keV}$$

$$V^0_{ff_{5/2}}(\text{KB3G}) = V^0_{ff_{5/2}}(\text{KB3}) - 150\text{keV}, \quad V^1_{ff_{5/2}}(\text{KB3G}) = V^1_{ff_{5/2}}(\text{KB3}) - 100\text{keV}$$

$$V^T_{pp}(\text{KB3G}) = V^T_{pp}(\text{KB3}) + 400\text{keV}$$

$p \ldots p_{3/2}$ or $p_{1/2}$

	KB	KB3	KB3G	Exp.
$\Delta(^{48}\text{Ca})$ (MeV)	2.16	5.26	4.73	4.81
$\Delta(^{56}\text{Ni})$ (MeV)	3.52	8.57	7.12	6.39

$$\Delta(^{48}\text{Ca}) = 2BE(^{48}\text{Ca}) - BE(^{49}\text{Ca}) - BE(^{47}\text{Ca})$$

$$\Delta(^{56}\text{Ni}) = 2BE(^{56}\text{Ni}) - BE(^{57}\text{Ni}) - BE(^{55}\text{Ni})$$

KB3G

FDA*

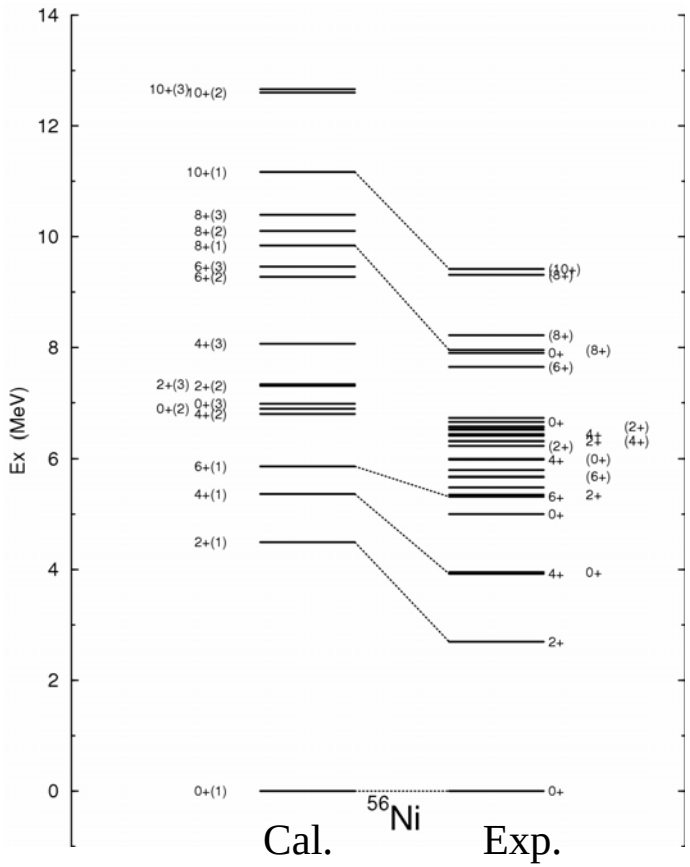
Ex (MeV)
14
12
10
8
6
4
2
0
10+(3)
10+(2)
10+(1)
8+(3)
8+(2)
8+(1)
6+(3)
6+(2)
4+(3)
2+(3)
2+(2)
0+(2)
0+(3)
4+(2)
6+(1)
4+(1)
2+(1)
0+(1)
(10+)
(8+)
(8+)
0+
(6+)
0+
4+
(2+)
(2+)
4+
(0+)
(6+)
6+
2+
0+
4+
0+
2+
0+
56Ni
Cal.
Exp.

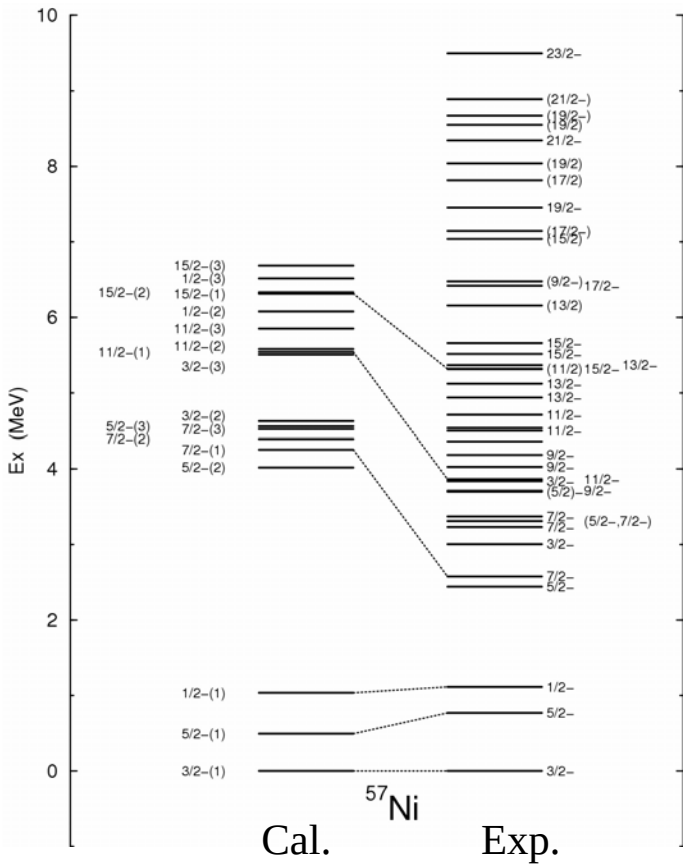
Ex (MeV)
10
8
6
4
2
0
15/2−(3)
1/2−(3)
15/2−(2)
15/2−(1)
1/2−(2)
11/2−(3)
11/2−(2)
11/2−(1)
3/2−(3)
3/2−(2)
5/2−(3)
7/2−(3)
7/2−(2)
7/2−(1)
5/2−(2)
1/2−(1)
5/2−(1)
3/2−(1)
23/2−
(21/2−)
(19/2)
21/2−
(19/2)
(17/2)
19/2−
(15/2)
(9/2−)
17/2−
(13/2)
15/2−
15/2−
(11/2)
15/2−
13/2−
13/2−
13/2−
11/2−
11/2−
9/2−
9/2−
3/2−
11/2−
(5/2)−
9/2−
7/2−
7/2−
(5/2−,7/2−)
3/2−
7/2−
5/2−
1/2−
5/2−
3/2−
57Ni
Cal.
Exp.

GT- strength ^{58}Ni to ^{58}Cu

Y. Fujita et al., EPJ A13 (2002) 411

KB3G

t =4

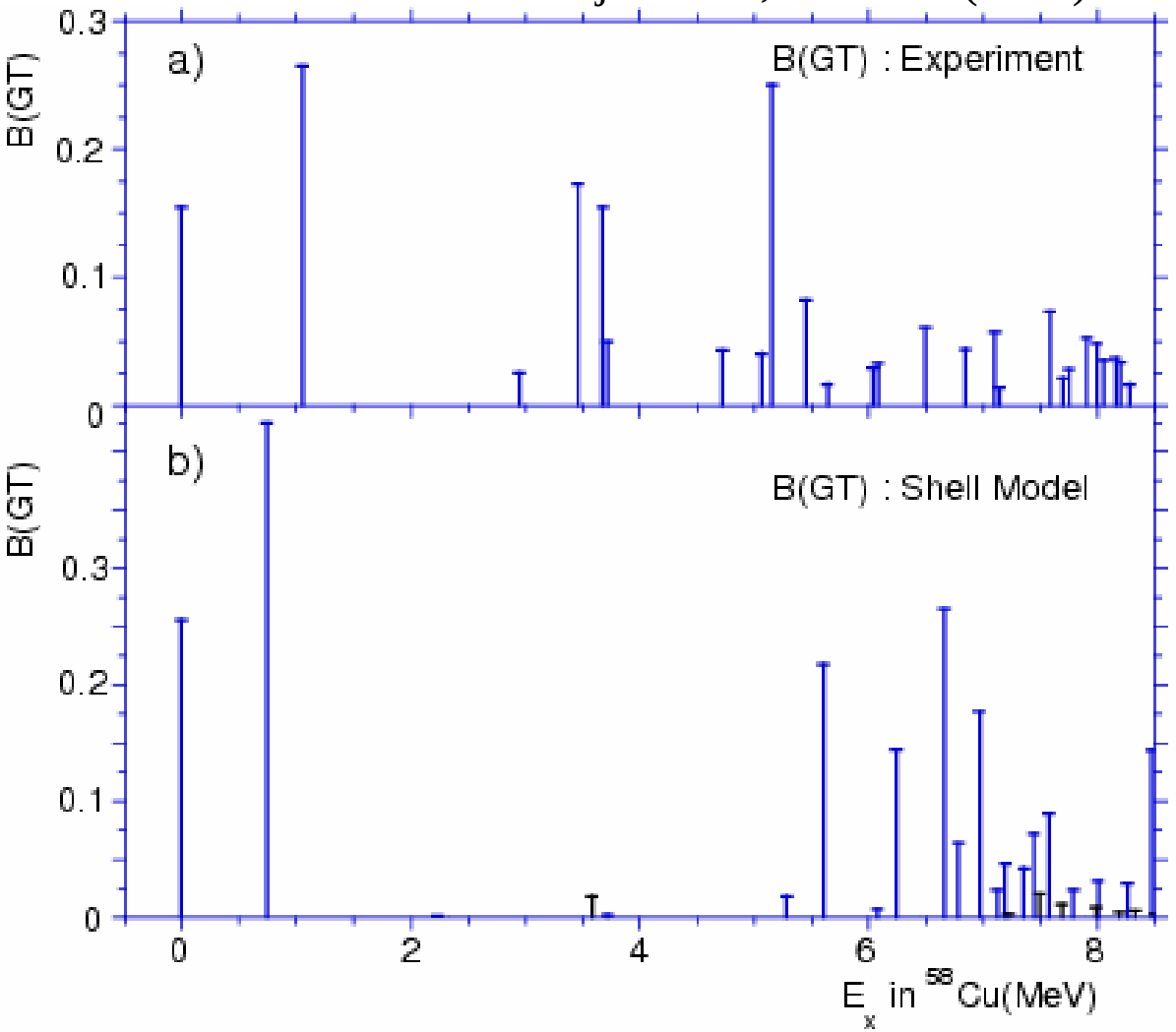

GXPF1 interaction

M. Honma et al., PRC65 (2002) 061301(R)

- Modify G interaction
- 195 TBME and 4 SPE are determined by fitting to 699 experimental energy data of 87 nuclei
- 70 well-determined LC's of parameters are varied
- Mass dependence

$$V(A) = V(A=42) \times \left(\frac{A}{42}\right)^{-0.3}$$

- Data selection to avoid intruder: $47 \leq A, \quad Z \leq 32$
- Energy evaluation by FDA* $\longrightarrow$ 168keV rms error

GXPF1 vs. KB3G

Estimated rms error (FDA*)

nuclei	states	rms error in MeV (# of data)	
		GXPF1	**KB3G**
N, Z<28	Yrast*)	0.154(136)	0.235(129)
	Yrare	0.201(45)	0.263(23)
N or Z=28	Yrast*)	0.184(92)	0.647(87)
	Yrare	0.195(57)	0.802(44)
N>28, Z<28	Yrast*)	0.145(129)	0.296(126)
	Yrare	0.145(75)	0.302(55)
N, Z>28	Yrast*)	0.186(55)	0.401(51)
	Yrare	0.187(23)	0.458(23)

*) Ground states are excluded

GXPF1

- MCSM (~13 bases / each level)
- $(f_{7/2})^{16}$ prob. in g.s. 69%

  cf. $(f_{7/2})^{8}$ in ^{48}Ca g.s. 94%
- ○ Members of 4p-4h band

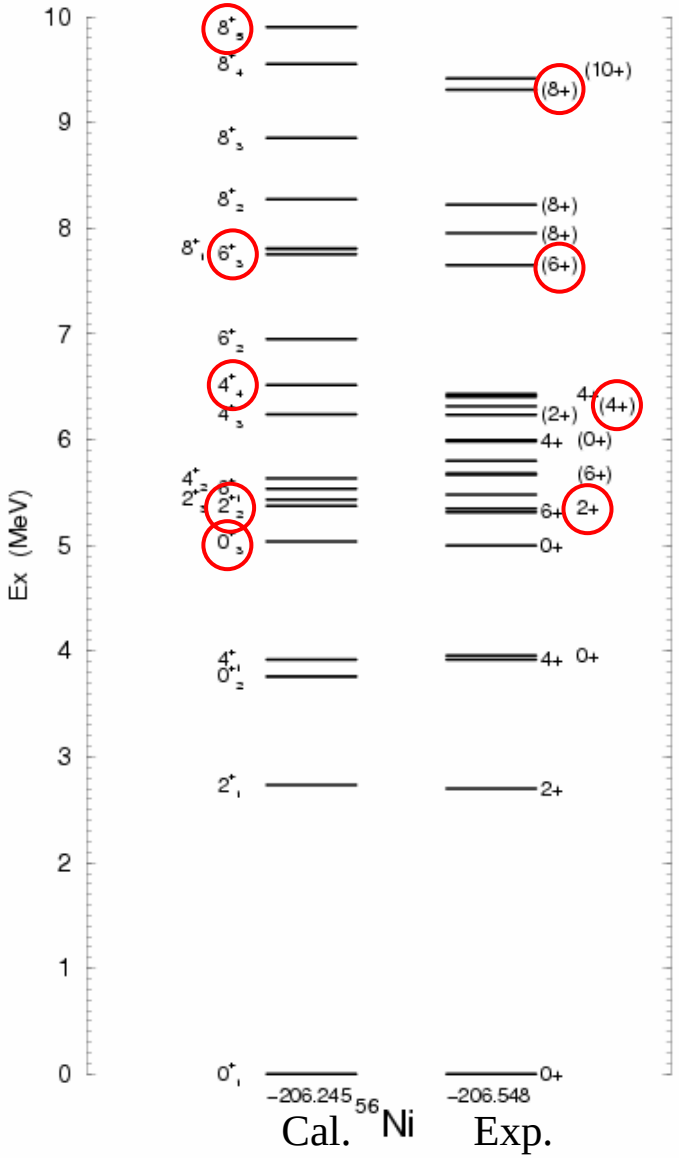

GXPF1

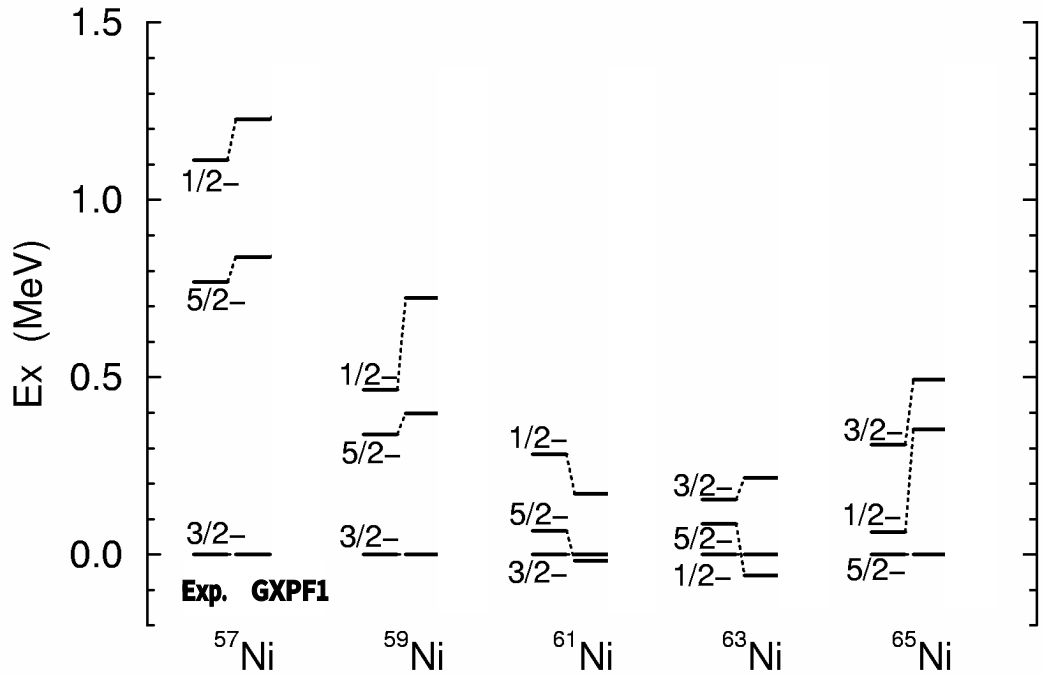
Ex (MeV)
1.5
1.0
0.5
0.0
Exp. GXPF1
1/2–
5/2–
3/2–
^{57}Ni
^{59}Ni
^{61}Ni
^{63}Ni
^{65}Ni

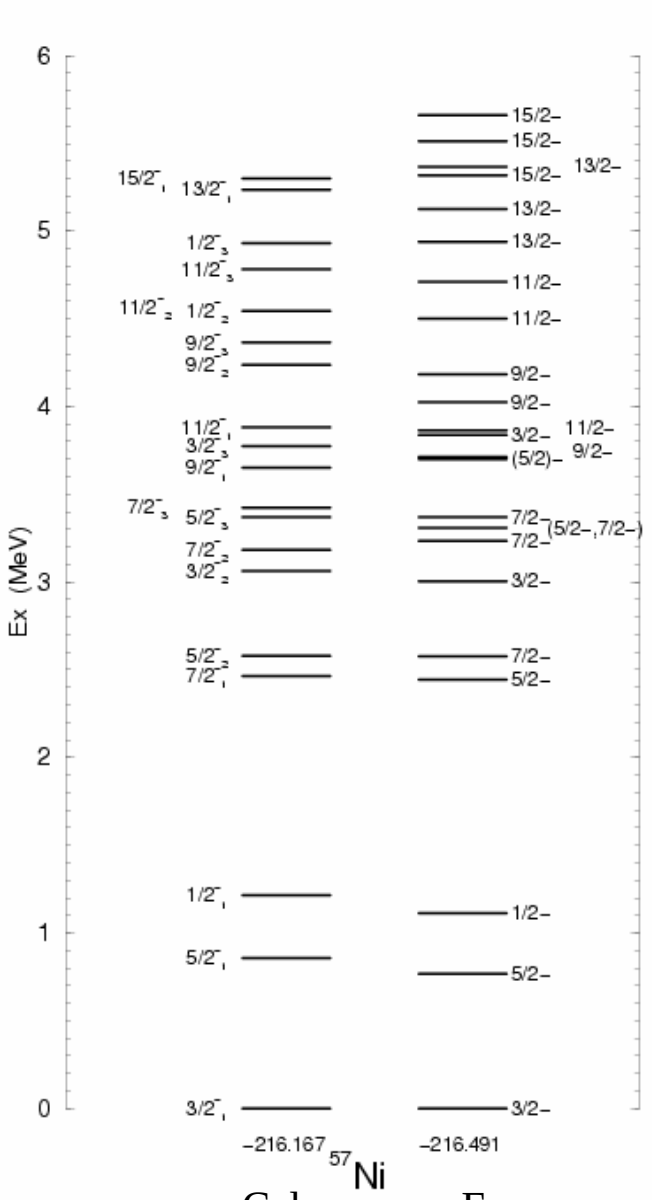
Ex (MeV)
6
5
4
3
2
1
0
−216.167 ^{57}Ni
−216.491
Cal.
Exp.

Binding energies

Empirical Coulomb energy

$$E_C = V_{\pi\pi}\frac{\pi(\pi-1)}{2} - V_{\pi\nu} + e_\pi \pi \qquad \pi, \nu \mathrm{L} \text{ valence nucleon \#}$$

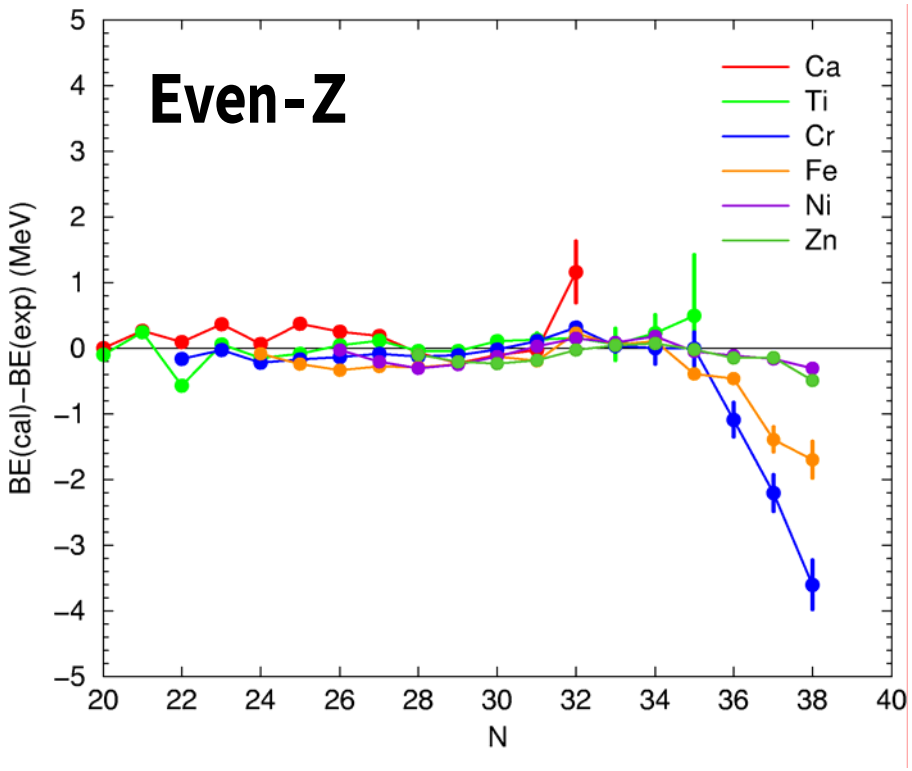

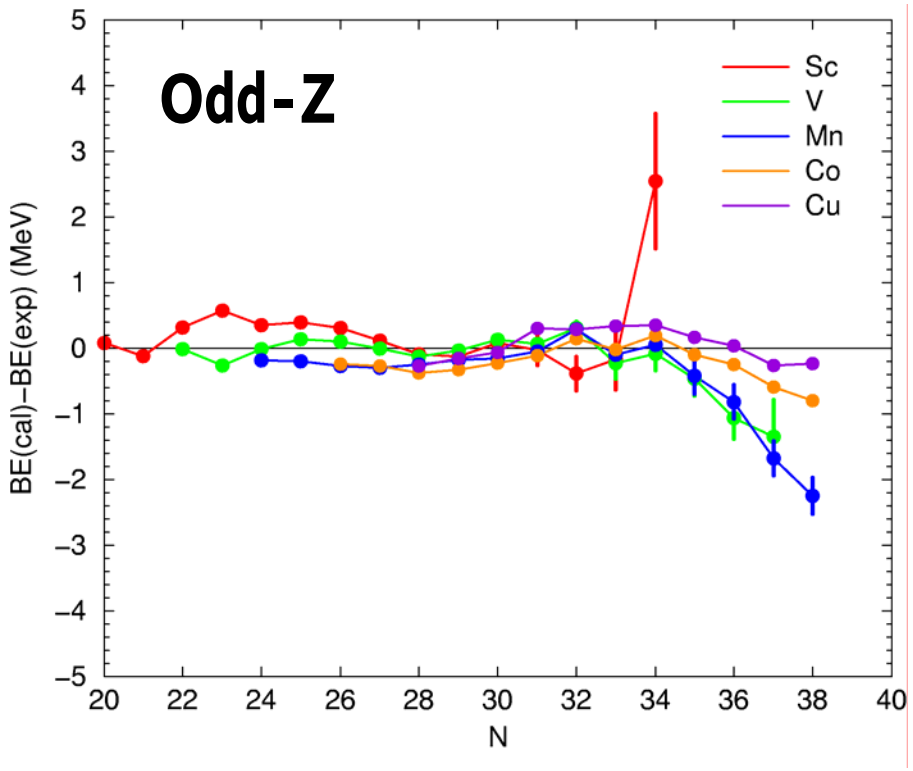

Electro-magnetic moments

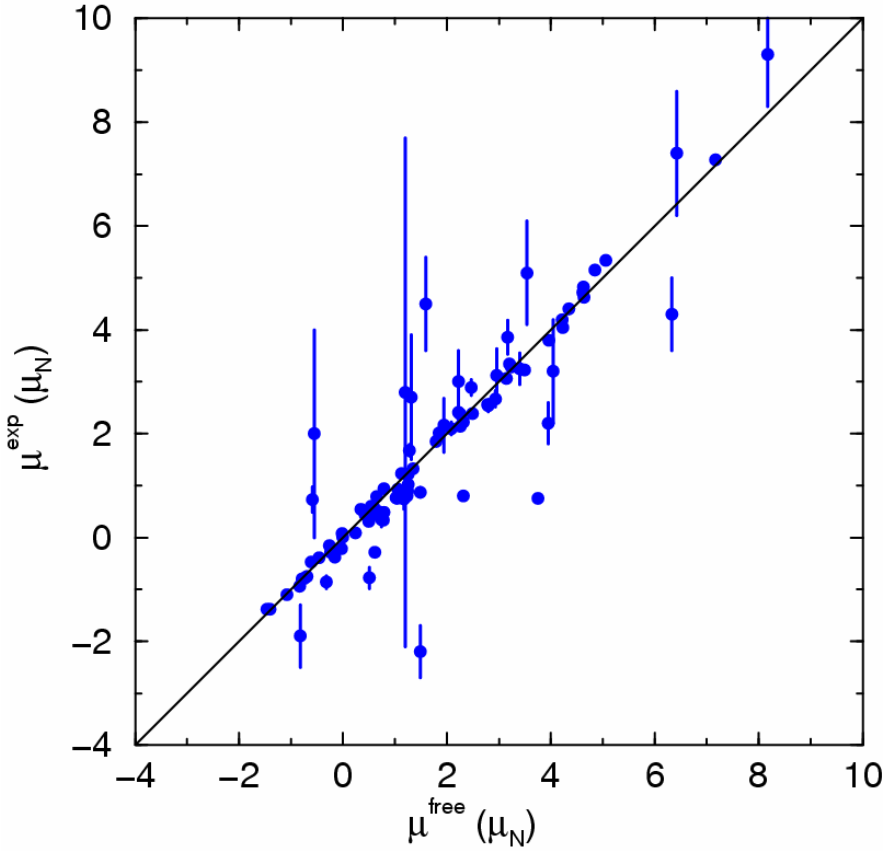

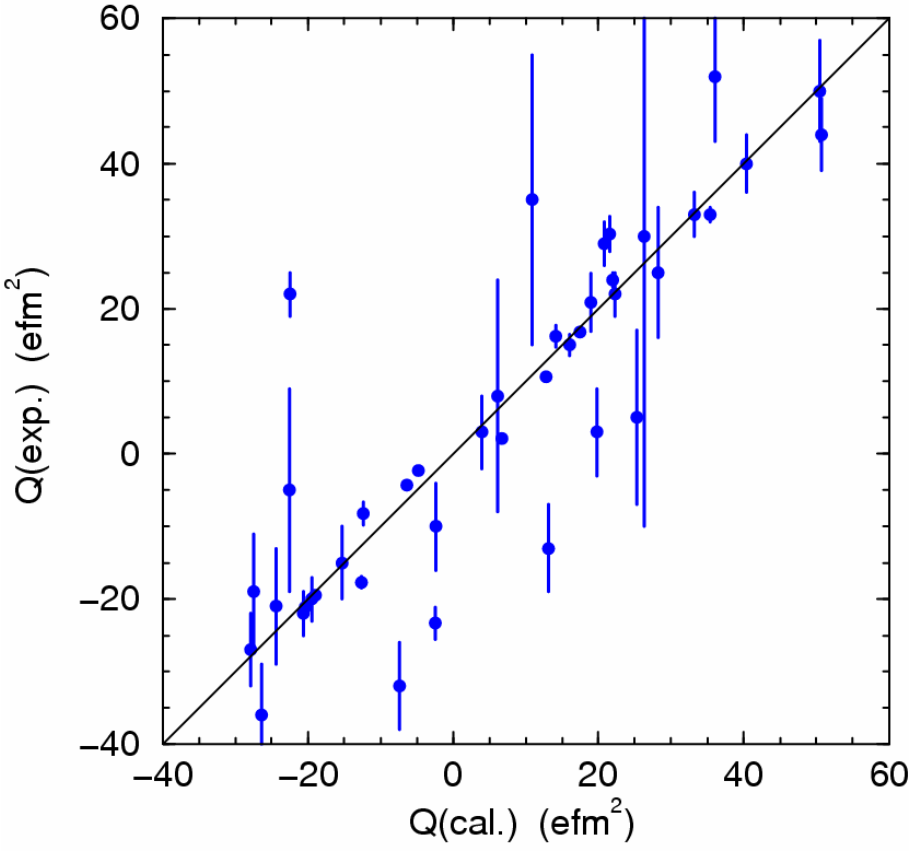

GT- strength ^{58}Ni to ^{58}Cu

GXPF1

$t = 5$

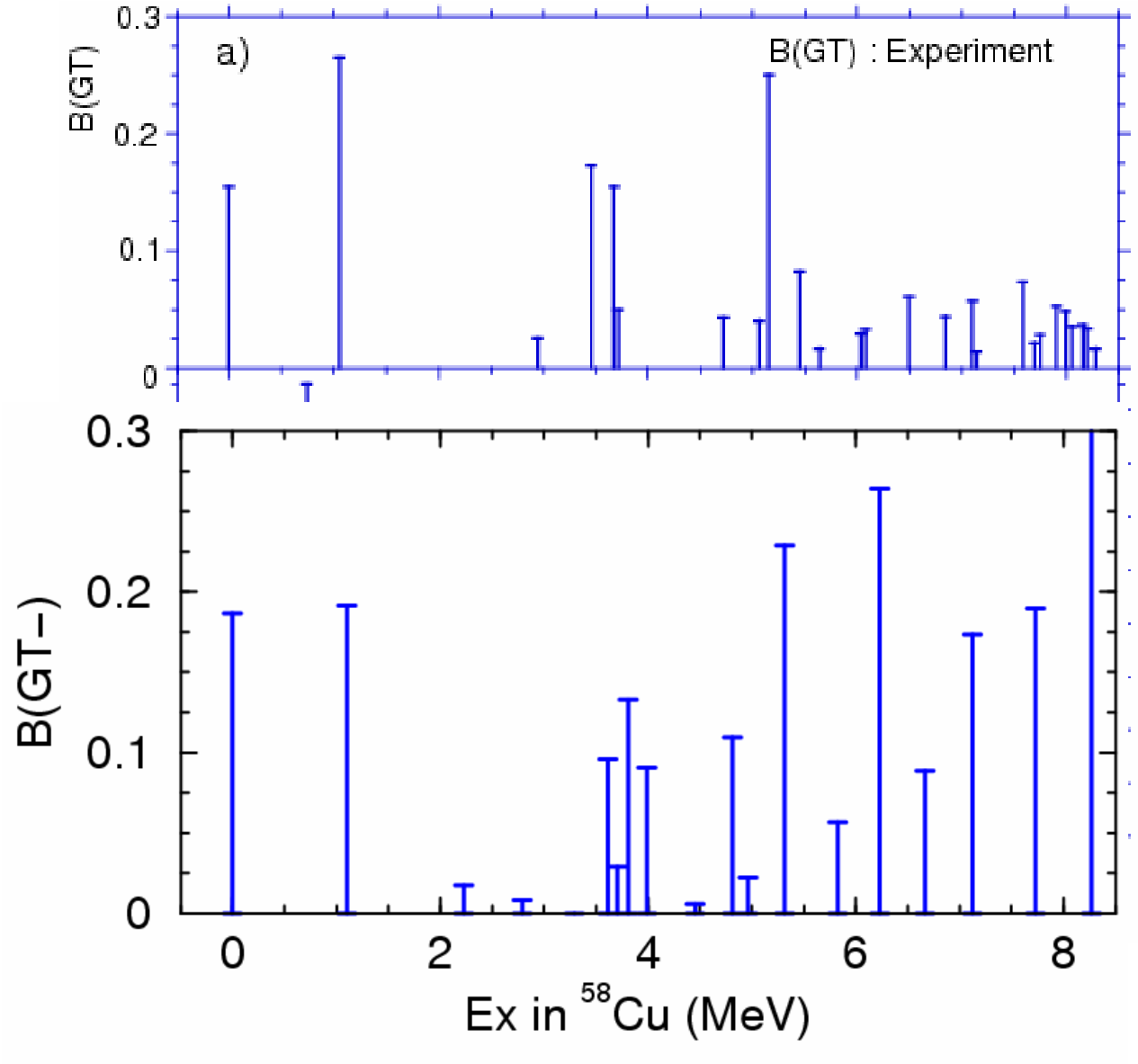

G vs. GXPF1

$V(abcd\,;\,JT)$

⇩

$abcd\,;\,JT$

$7=f_{7/2},\ 3=p_{3/2},\ 5=f_{5/2},\ 1=p_{1/2}$

- T=0 … attractive
- T=1 … repulsive
- Large modifications in

  $V(abab\,;\,J0)$ with large J

  $V(aabb\,;\,J1)$ pairing

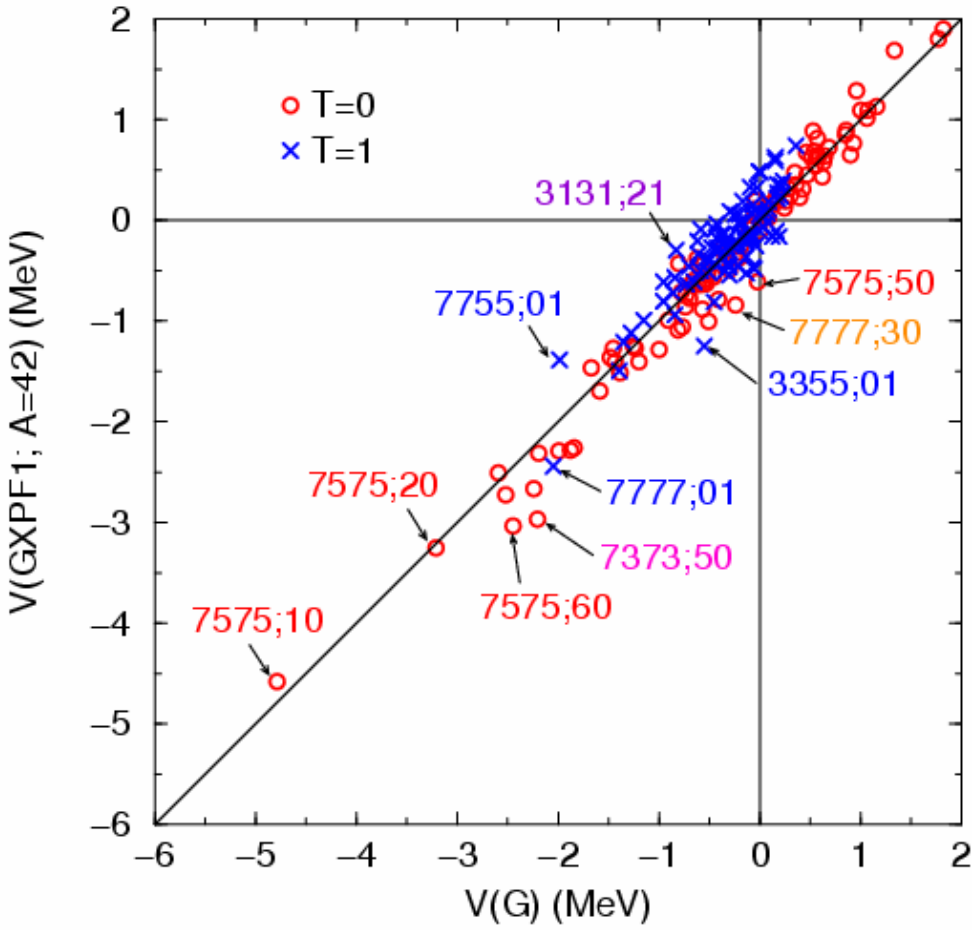

J-dependent modification

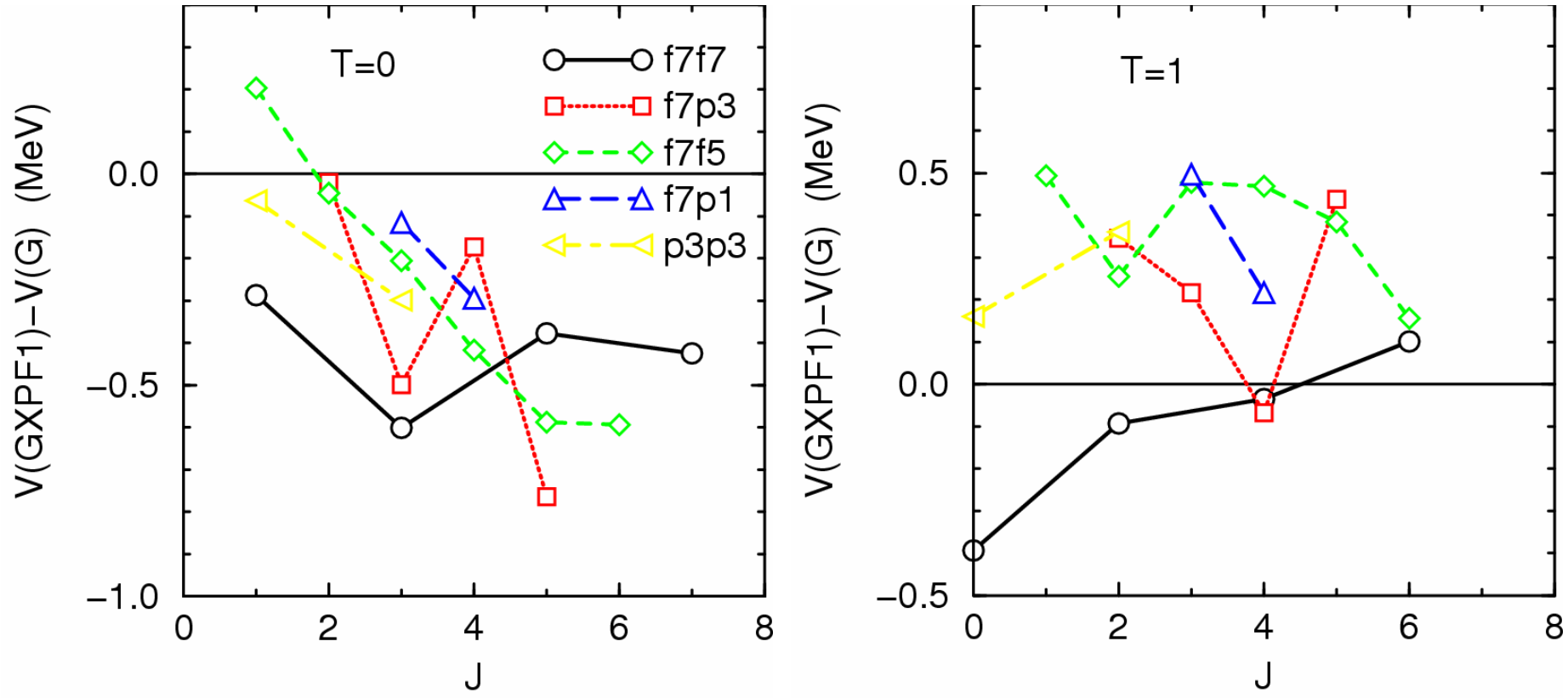

Monopole centroids

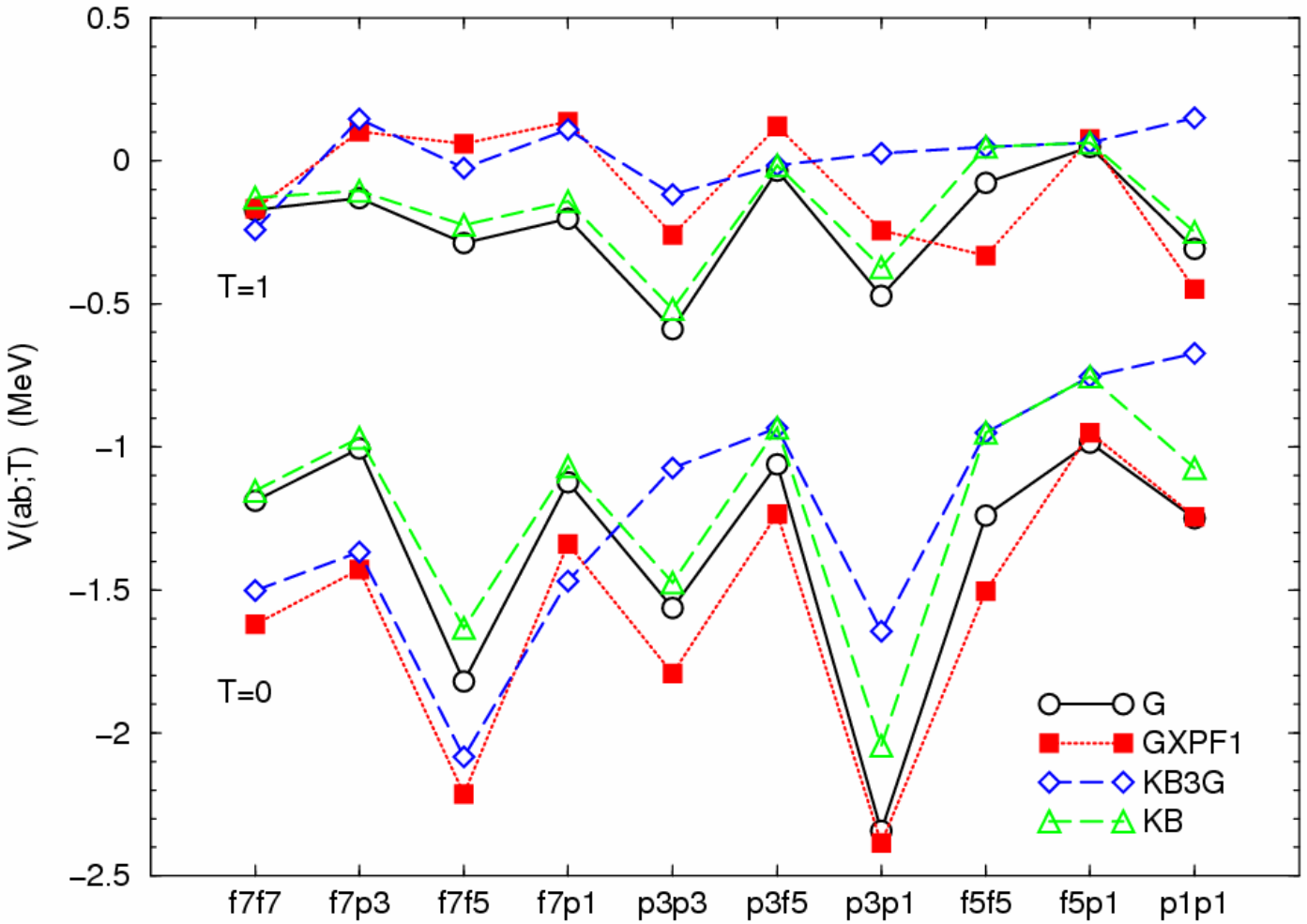

Effective single-particle energy (ESPE)

Y. Utsuno et al., PRC60 (1999) 054315

- Assume the lowest filling configuration
- Evaluate energy difference by H_m due to
  - removing one nucleon from an occupied orbit
  - adding one nucleon to an empty orbit

GXPF1

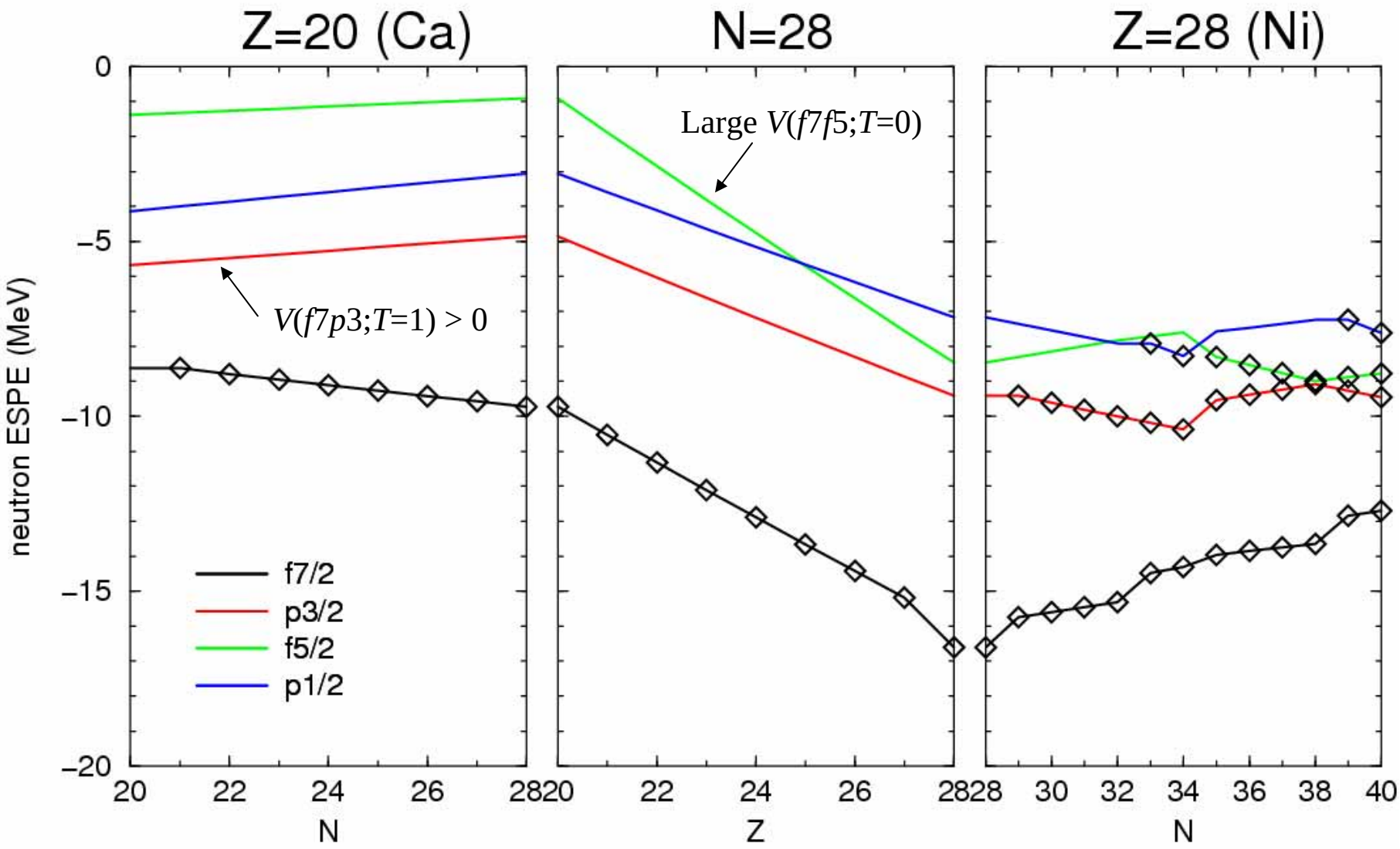
Z=20 (Ca)
N=28
Z=28 (Ni)
neutron ESPE (MeV)
0
−5
−10
−15
−20
Large V(f7f5;T=0)
V(f7p3;T=1) > 0
f7/2
p3/2
f5/2
p1/2
20
22
24
26
28
N
Z
30
32
34
36
38
40

G interaction

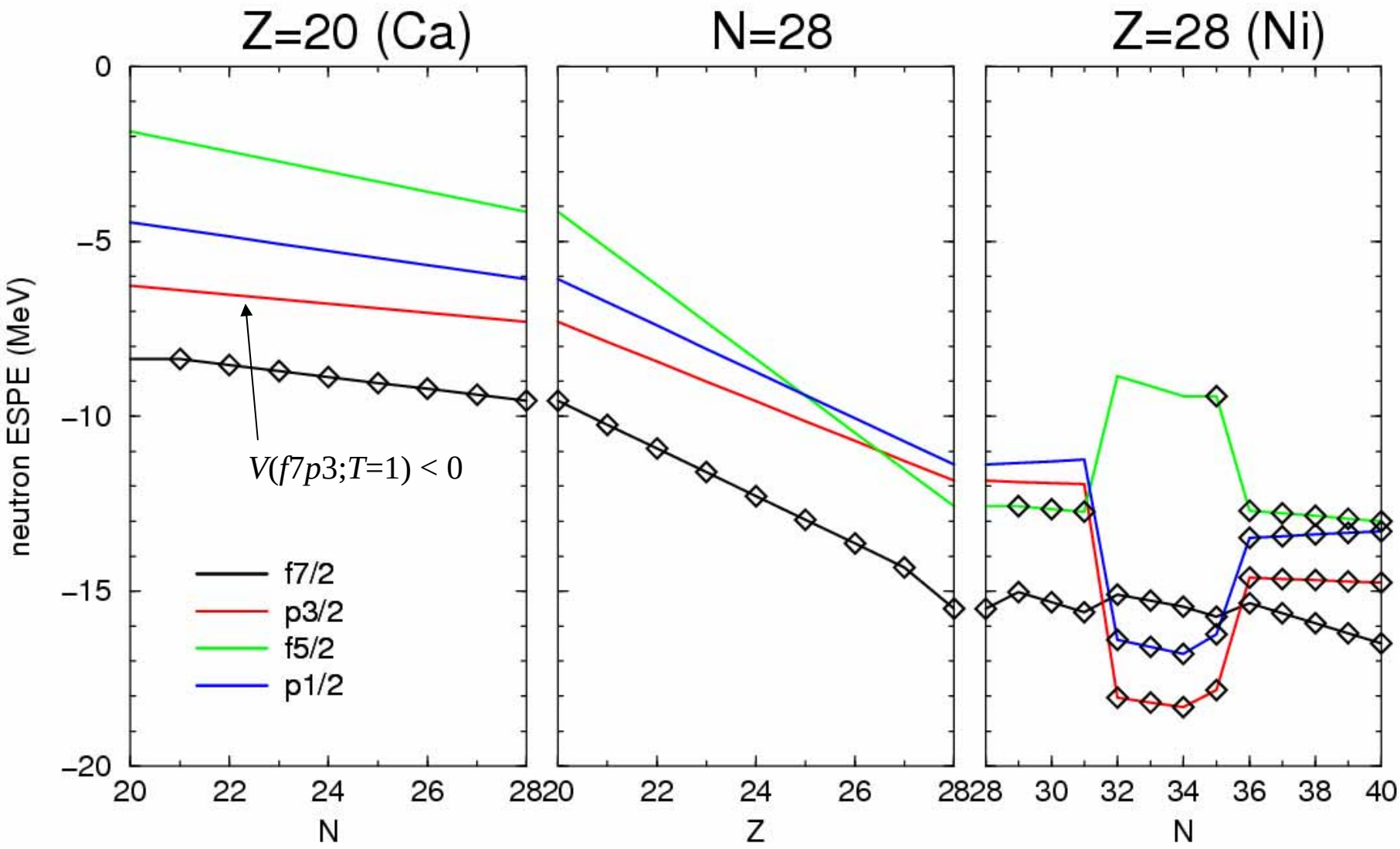

GXPF1

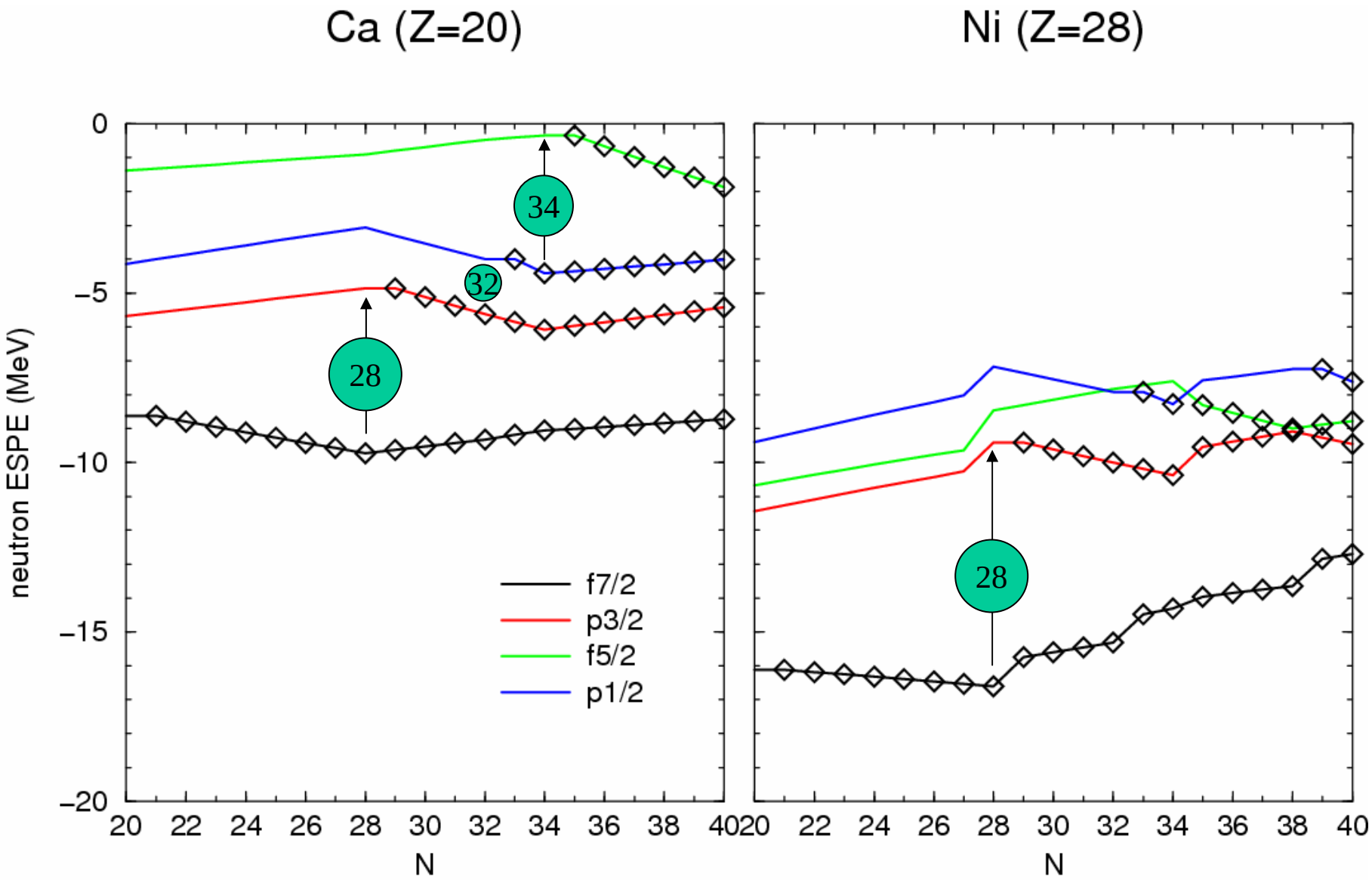
Ca (Z=20)
Ni (Z=28)
neutron ESPE (MeV)
0
−5
−10
−15
−20
20 22 24 26 28 30 32 34 36 38 40
N
34
32
28
28
f7/2
p3/2
f5/2
p1/2

Multipole Hamiltonian

Decomposition of Hamiltonian

$$H = H_m \text{ (monopole)} + H_M \text{ (multipole)}$$

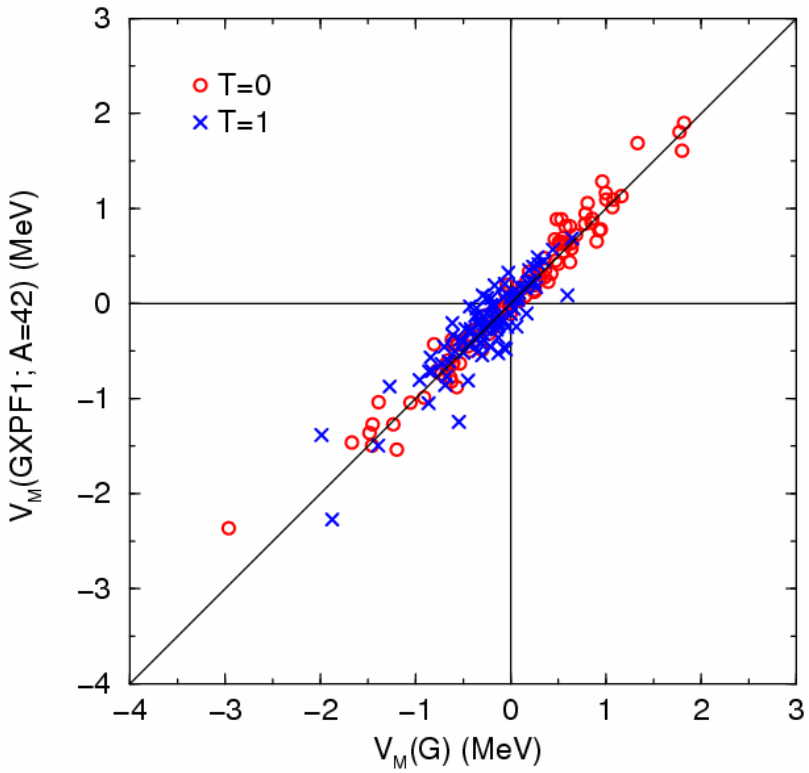

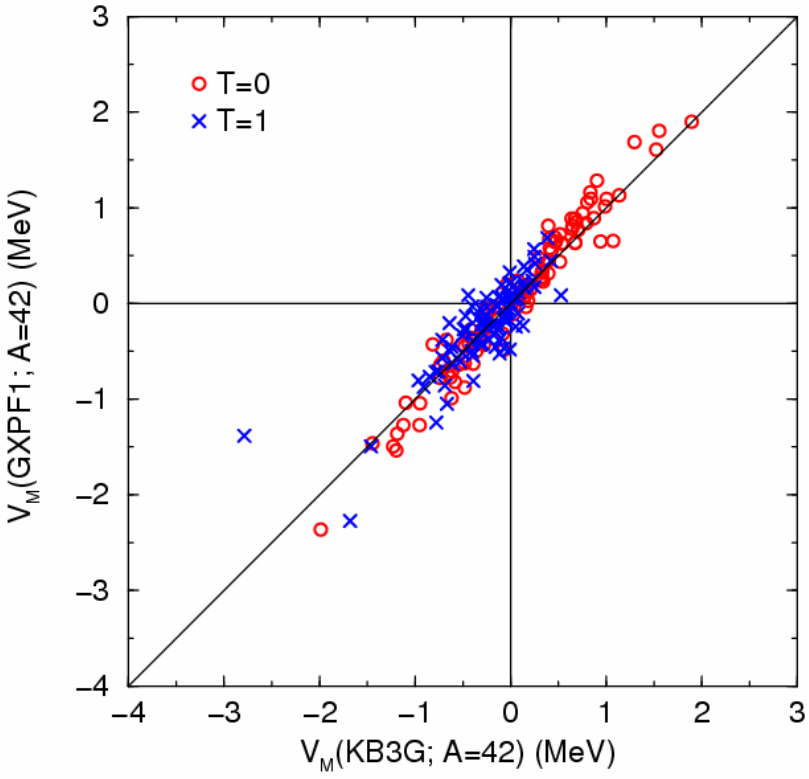

G vs. KB

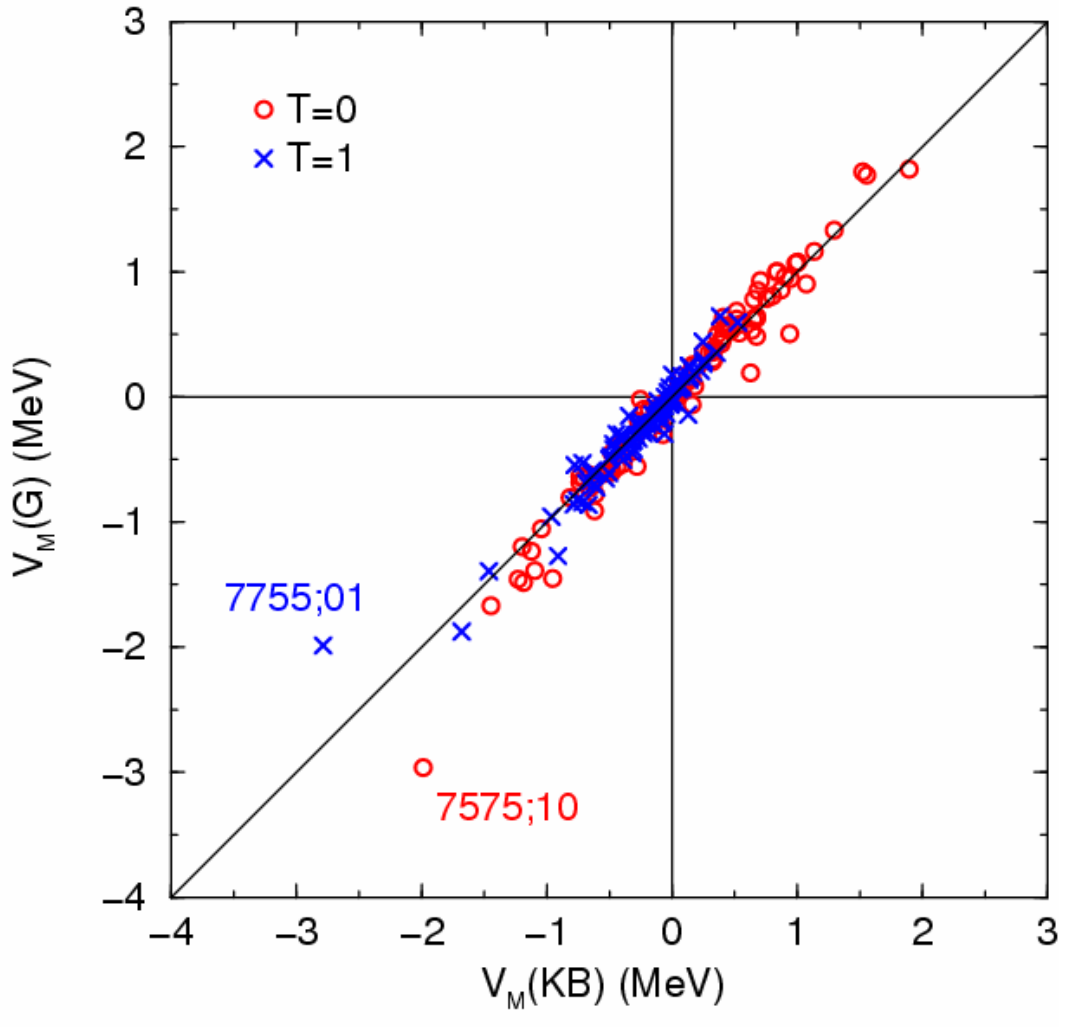

Collective properties

M. Dufour et al., PRC54 (1996) 1641

- Particle-particle (p-p) representation
  - Diagonalize $V(abcd;JT)$ matrix in terms of p-p bases

$$H_M = \sum_{a\le b, c\le d, JT} V^{JT}_{abcd} A^{\dagger}_{abJT} A_{cdJT} \quad \Rightarrow \quad \sum_{JT\alpha} E^{JT}_{\alpha} P^{\dagger}_{JT\alpha} P_{JT\alpha}$$

$$A^{\dagger}_{abJT} = (1+\delta_{ab})^{-1/2} \left[c^{\dagger}_a c^{\dagger}_b \right]^{JT}$$

eigenvalue large for JT=01, 10

- Particle-hole (p-h) representation
  - Diagonalize $\boldsymbol{\omega}(acbd; \boldsymbol{\lambda}\ \boldsymbol{\tau})$ matrix in terms of p-h bases

$$H_M = \sum_{abcd, \lambda\tau} \omega^{\lambda\tau}_{acbd} S_{ac\lambda\tau} \cdot S_{bd\lambda\tau} \quad \Rightarrow \quad \sum_{\lambda\tau k} e^{\lambda\tau}_k Q_{\lambda\tau k} \cdot Q_{\lambda\tau k}$$

$$S_{ac\lambda\tau} = \left[c^{\dagger}_a \tilde{c}_c \right]^{\lambda\tau}$$

eigenvalue large for $\boldsymbol{\lambda}\ \boldsymbol{\tau}$ =20, 40, 11

Collective strength

- Empirical fit reduces E^{10} and e^{20}

  (cf. Attractive modifications to T=0 monopole terms)

- Pairing strength

  T=0 > T=1 in G and GXPF1

  T=0 < T=1 in KB3G (~ KB)

Interaction	E^{01}	E^{10}	E^{20}	e^{20}	e^{40}	e^{11}
G	–4.20	–5.61	–2.96	–3.33	–1.30	+2.70
GXPF1	–4.18	–5.07	–2.85	–2.92	–1.39	+2.67
KB3G	–4.75	–4.46	–2.55	–2.79	–1.39	+2.47

Spin-tensor decomposition

B. A. Brown et al., Ann. Phys. 182 (1988) 191

- *jj*-coupling to *LS*-coupling

$$\langle j_a j_b JT | V_M | j_c j_d JT \rangle \Rightarrow \langle l_a l_b LSJT | V_M | l_c l_d L'S'JT \rangle$$

- Decomposition in terms of tensor rank *k*

$$V_M = \sum_k V_k = \sum_k U^k \cdot X^k$$

U^k and X^k … irreducible tensors in space and spin

k=0 … central

k=1 … spin-orbit

normal part : $S = S' = 1$

anti-symmetric part: $S \neq S'$

k=2 … tensor

Central

- for T=0, G ~ GXPF1

  except for l=3, L=0

- for T=1, large correction to

  l=3, L=0 and 2

- G and KB3G are different

  in T=0, S=0

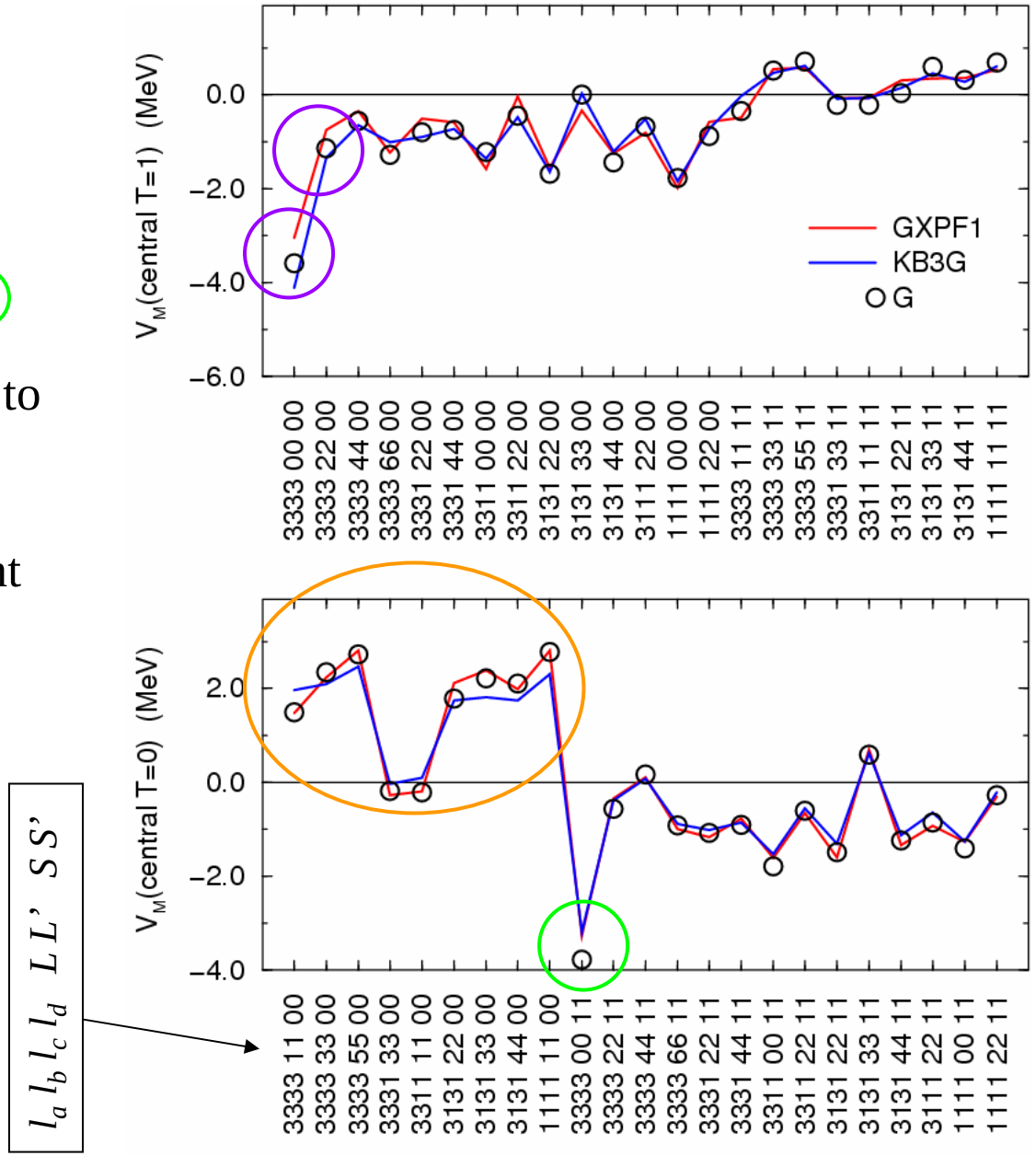

Tensor

- large in T=0, ΔL=2 m.e.
- for T=1, G ~ GXPF1

  except for a few m.e.
- for T=0, corrections to G is

  not large.
- G and KB3G are different

  in several large T=0 m.e.,

  while they are very close

  for T=1 m.e.

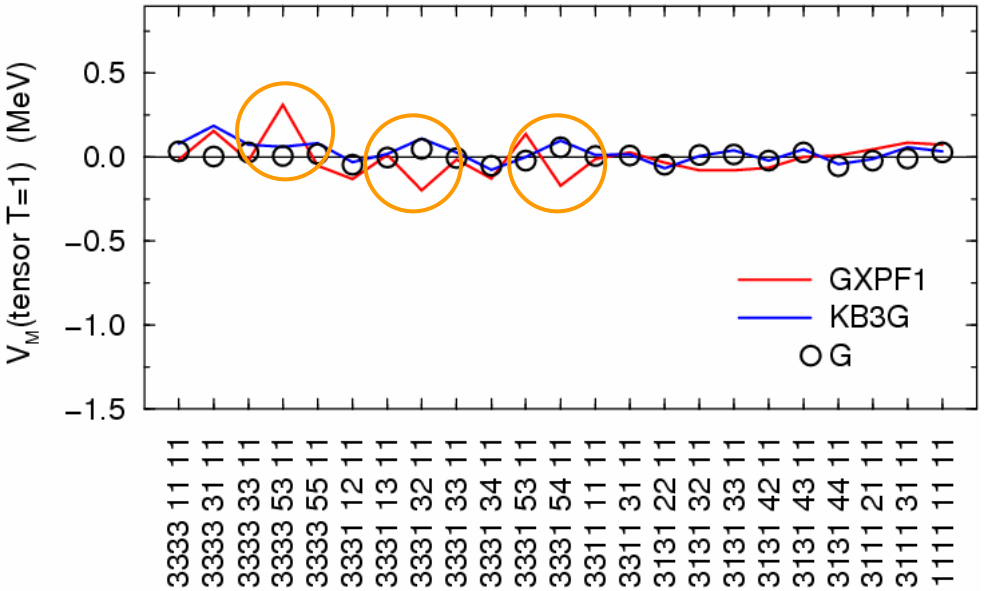

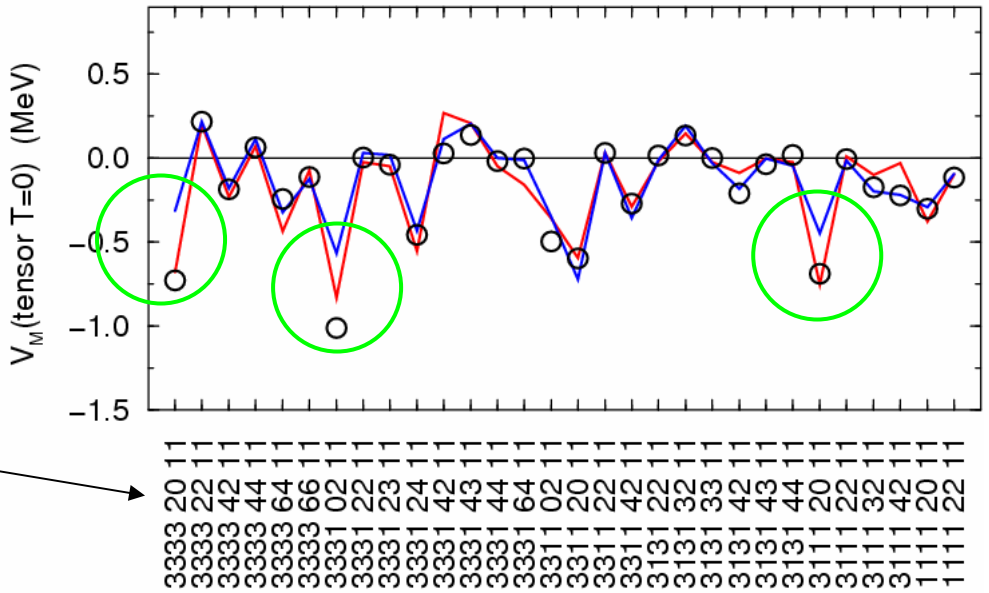

$l_a\, l_b\, l_c\, l_d \quad L\, L' \quad S\, S'$

Spin-orbit (normal)

- Several corrections to G, ○ which are absent in KB3G
- G ~ KB3G

  except for T=0, l=3, L=2 ○

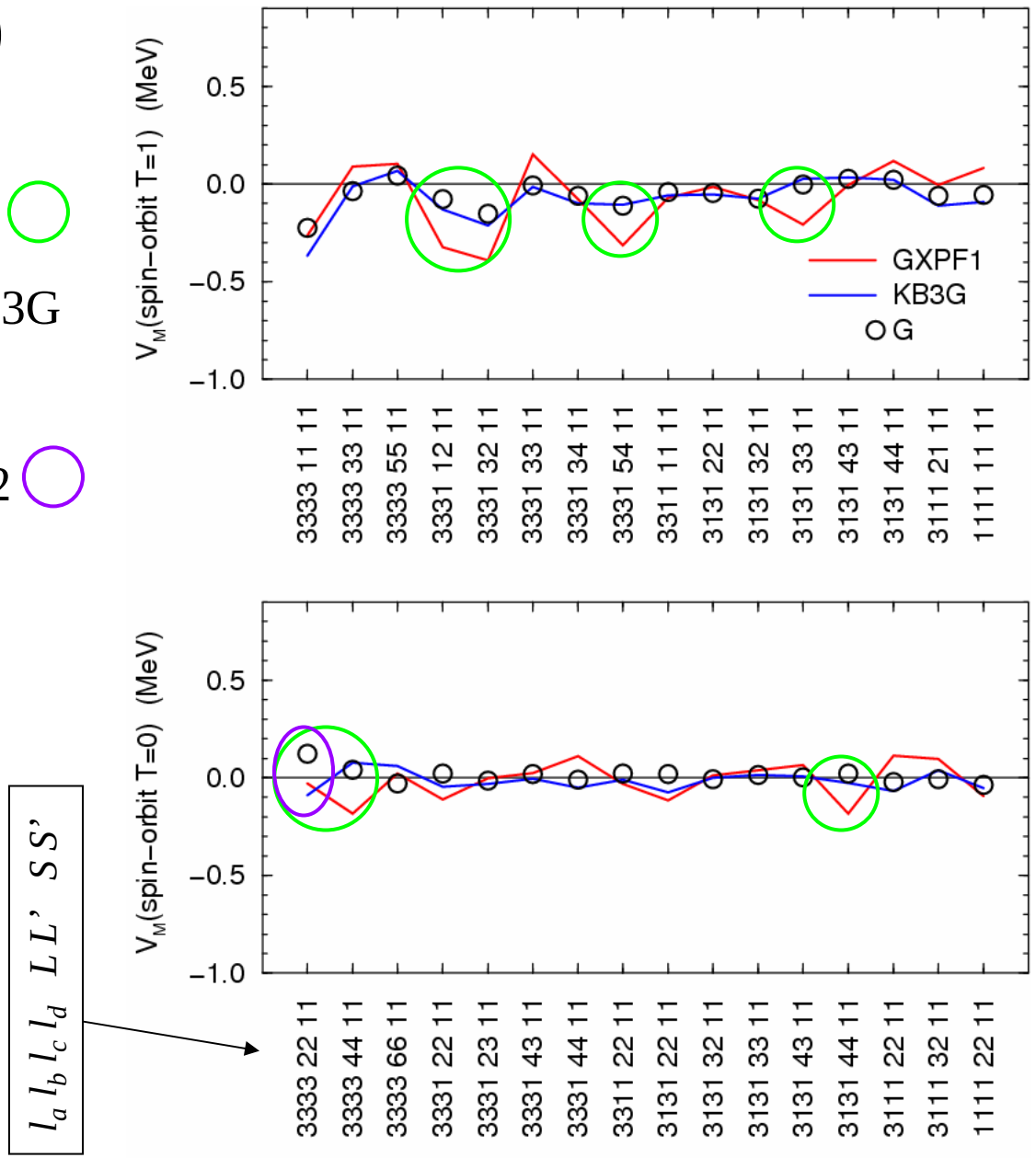

Spin-orbit (anti-sym.)

- M.e. are small
- Several corrections to G,

  which are absent in KB3G
- G ~ KB3G

  with a few exceptions

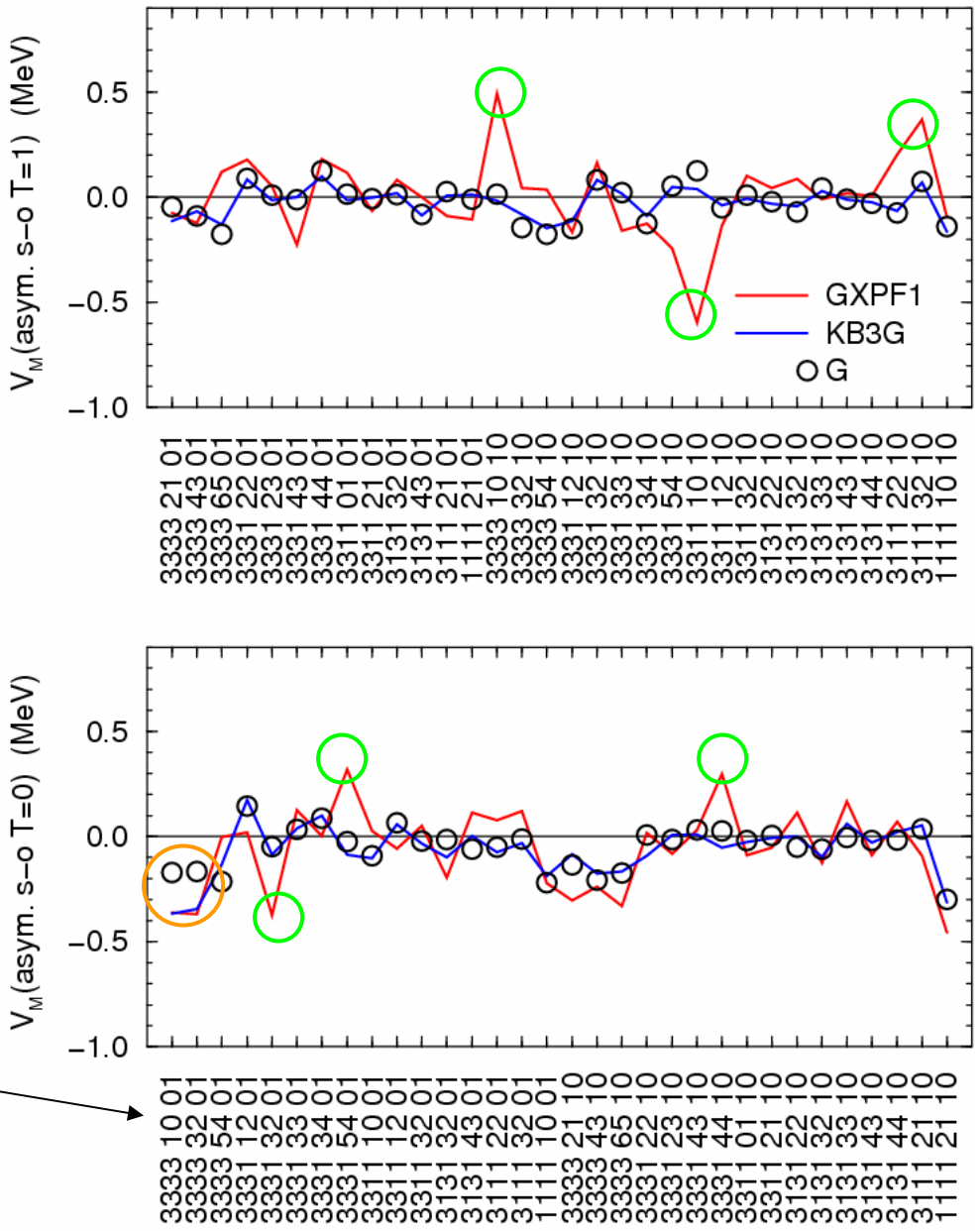

GXPFM interaction

- Start from G interaction
- Vary 70 parameters
  - Monopole — 20 TBME+4 SPE
  - Monopole pairing (JT=01) — 10 TBME
  - Quadrupole pairing (JT=21) — 36 TBME
- Mass dependence $A^{-0.3}$
- Adopt 45 best determined LC's
- Fit to 623 energy data $\longrightarrow$ rms error 226 keV by FDA*
  - 267 keV (yrast, 87 data) and 324 keV (yrare, 44 data) for N or Z=28 nuclei … not very good!

Shell gap

	GXPF1	GXPFM	KB3G	Exp.
$\Delta(^{48}\mathrm{Ca})$ (MeV)	4.97	4.66	4.73	4.81
$\Delta(^{56}\mathrm{Ni})$ (MeV)	7.58	6.91	7.12	6.39

Collective strength

Interaction	E^{01}	E^{10}	E^{20}	e^{20}	e^{40}	e^{11}
G	–4.20	–5.61	–2.96	–3.33	–1.30	+2.70
GXPF1	–4.18	–5.07	–2.85	–2.92	–1.39	+2.67
GXPFM	–3.88	–5.61	–2.96	–2.85	–1.44	+2.59

Monopole centroid

G vs. GXM

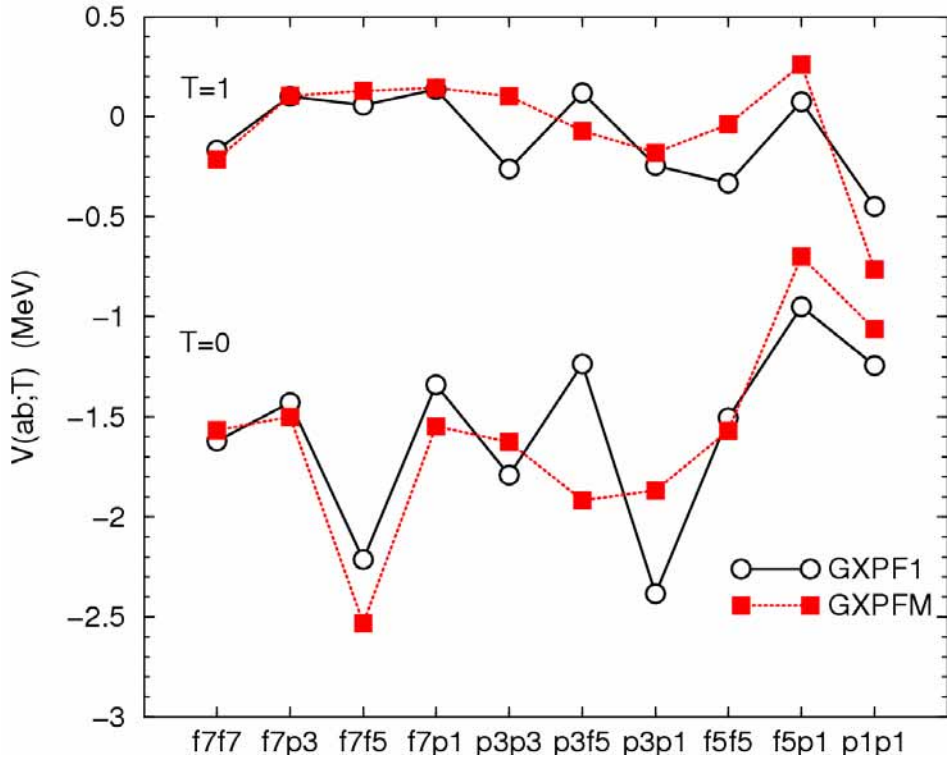

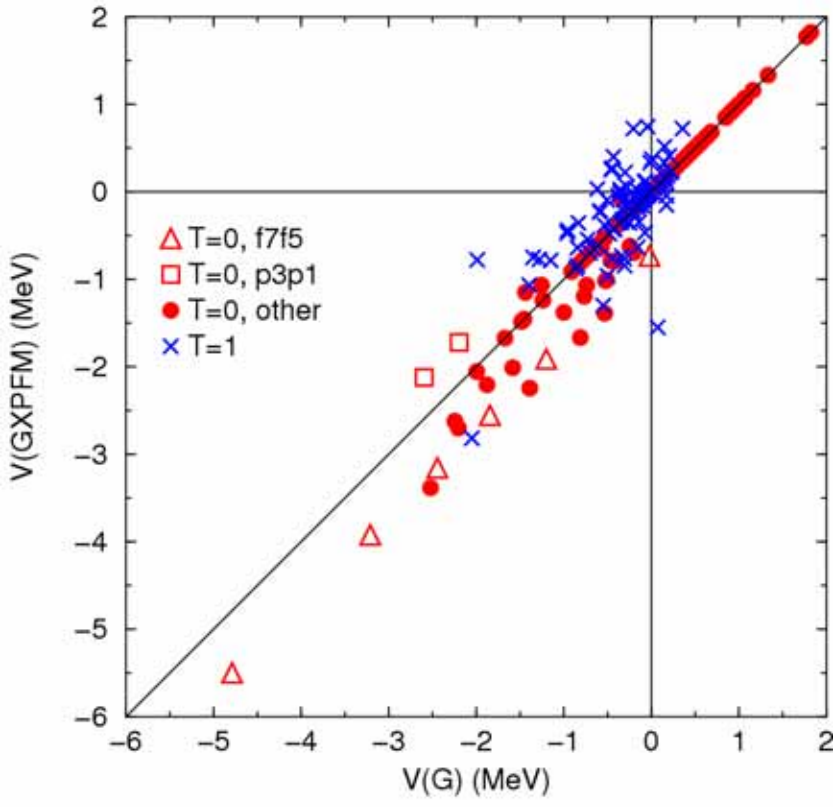

Core excitation

- Apparent in semi-magic nuclei
- Difficulties in “monopole-corrected” interactions

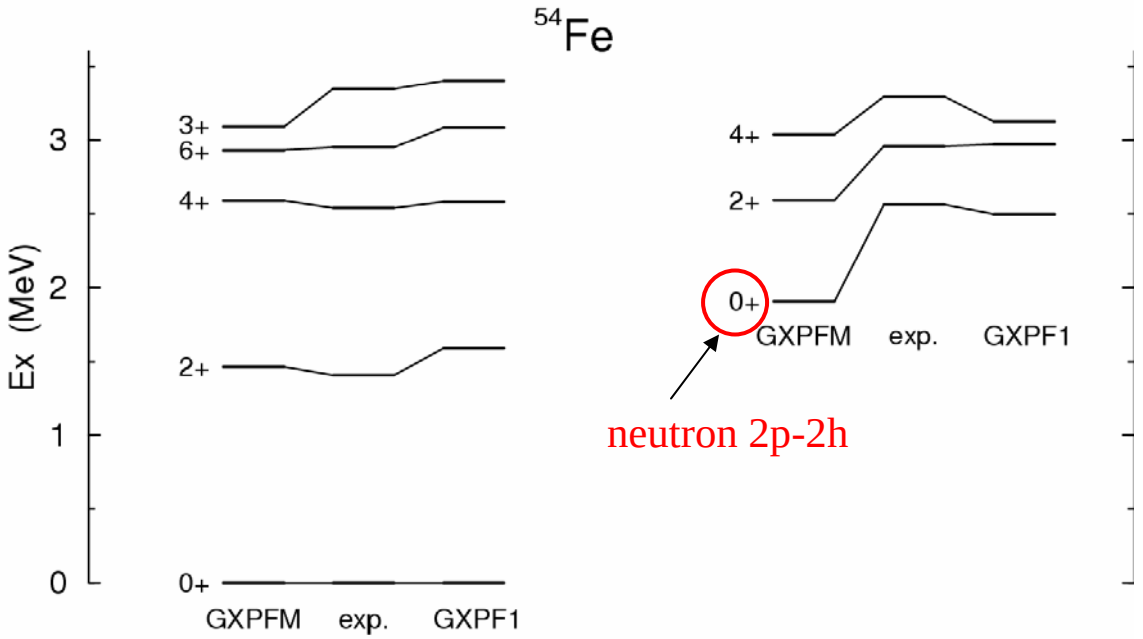

$^{56,\ 57}$Ni problem

Modify $V(7373; J1)$

– J=4 –300keV

– J=5 +250keV

(Monopole centroid is unchanged)

GXPFM ⟶ GXPFM’

KB3G ⟶ KB3G’

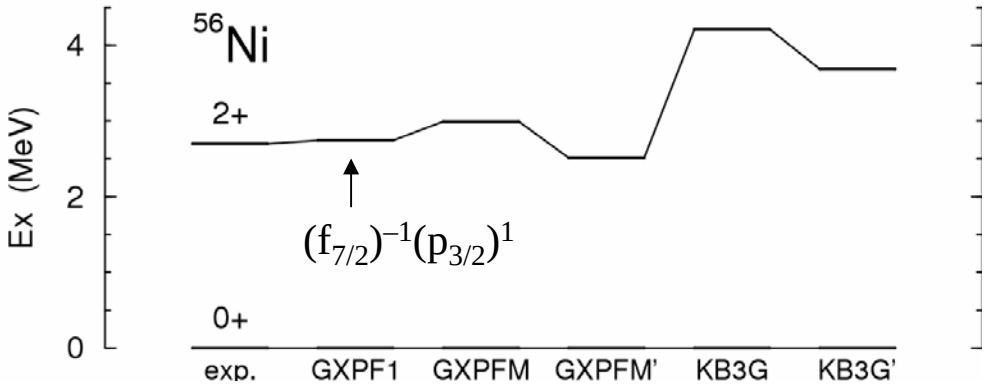

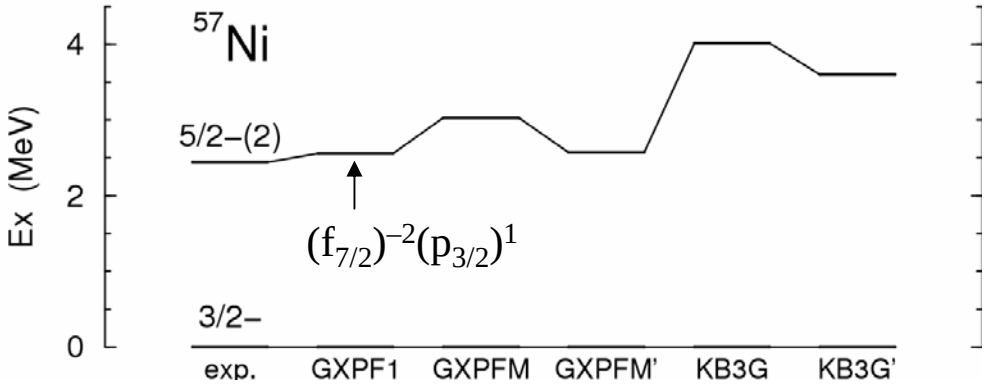

Quadrupole modification

$$\left[c^{\dagger}_{f\,7/2}\tilde{c}_{p3/2}\right]^{(2)}\cdot\left[c^{\dagger}_{p3/2}\tilde{c}_{f\,7/2}\right]^{(2)}$$

term strength (MeV)

- GXPF1 –0.81
- G –0.38
- GXPFM –0.32
- KB3G –0.34

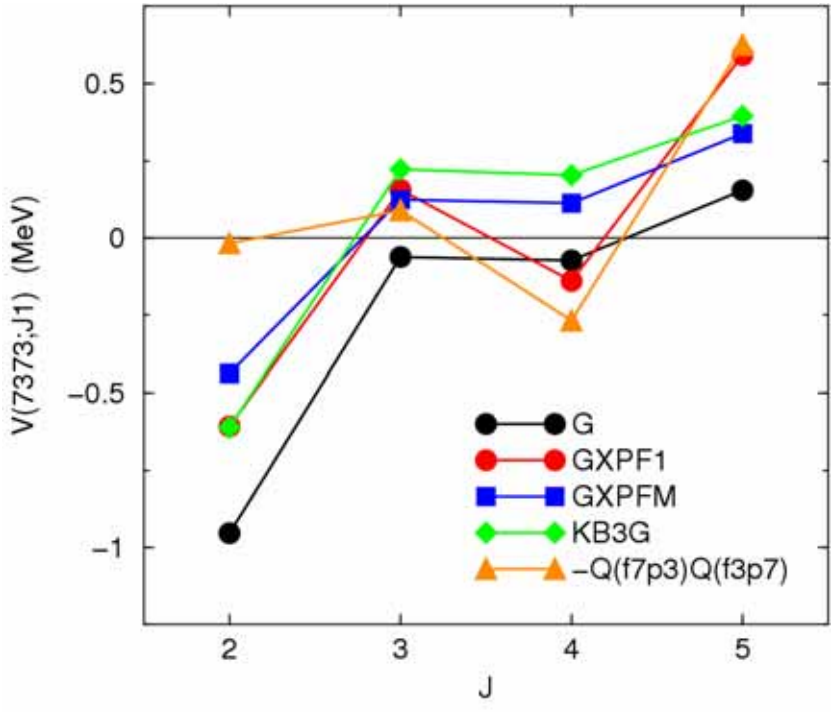

Summary

- Microscopic interaction can be modified for a practical use
  - $T=0$ … more attractive
  - $T=1$ … more repulsive
- Monopole modification is important, but not enough
  - Pairing strength
  - Quadrupole-quadrupole strength
- Fitting to exp. energy data gives reasonable modification
- Prospects
  - General rule for modifying microscopic interactions
  - Microscopic origin of modifications